Received: 18 January 2021 | Revised: 8 March 2021 | Accepted: 9 March 2021

DOI: 10.1002/jhet.4260

ARTICLE

JOURNAL OF HETEROCYCLIC CHEMISTRY WILEY

Synthesis, structural characterization, biological activity, and theoretical studies of some novel thioether-bridged 2,6-disubstituted imidazothiadiazole analogues

Hasan Tunel[1] | **Mustafa Er**[1] | **Hakan Alici**[2] | **Abdurrahman Onaran**[3] | **Tuncay Karakurt**[4] | **Hakan Tahtaci**[1]

[1]Department of Chemistry, Faculty of Science, Karabuk University, Karabuk, Turkey

[2]Department of Physics, Faculty of Arts and Sciences, Zonguldak Bulent Ecevit University, Zonguldak, Turkey

[3]Department of Plant and Animal Production, Kumluca Vocational School of Higher Education, Akdeniz University, Antalya, Turkey

[4]Department of Chemical Engineering, Faculty of Engineering and Architecture, Kirsehir Ahi Evran University, Kirsehir, Turkey

Correspondence
Hakan Tahtaci, Department of Chemistry, Faculty of Science, Karabuk University, 78050, Karabuk, Turkey.
Email: hakantahtaci@karabuk.edu.tr

Funding information
Karabük Üniversitesi, Grant/Award Number: KBU-BAP-16/2-YL-090

In this study, thioether-bridged imidazo[2,1-*b*][1,3,4]thiadiazole derivatives that contained both imidazole and 1,3,4-thiadiazole (compounds **7a-7i** and **8a-8i**) were synthesized from the reactions of 2-amino-1,3,4-thiadiazole with phenacyl bromide (**6a-6i**) (at yields of 59% to 74%). The structure of the synthesized compounds was characterized using ^{1}H NMR, ^{13}C NMR, Fourier-transform infrared spectroscopy, elemental analysis, mass spectroscopy, and X-ray diffraction analysis. Mycelial growth, mycelial growth inhibition, minimum inhibitory concentration, minimum fungicidal concentration, and lethal dose values against various plant pathogenic fungi were determined for all of the target compounds synthesized in the study. The test results showed that most of the compounds had moderate to good antifungal activity. In addition, the absorption, distribution, metabolism, excretion (ADME) parameters of the compounds were calculated, and it was observed that all of the compounds met the drug-likeness rules in general. Finally, using docking simulations, it was found that compounds **7h**, **7i**, **8h**, and **8i** showed high affinity to PDB ID:5TZ1, which is an CYP51 antifungal target structure.

1 | INTRODUCTION

In recent years, interest in antimicrobial drugs has been growing due to such reasons as the increasing prevalence of viral diseases, high toxicity of existing drugs, constantly mutating viruses, and factors related to various causes affecting the human immune system.[1] For these reasons, scientists are making great efforts to design novel drugs against constantly evolving diseases that have low cost, high efficiency, minimal toxicity, and maximal bioavailability. Heterocyclic compounds, which can be widely found in nature, as well as obtained by synthetic means, and are used in many industries, have an important place in human life.

These compounds are used as therapeutic agents in pharmaceutical chemistry and are found in the structures of many commercially available drugs.[2,3] The heterocyclic derivatives of imidazole ($C_3H_4N_2$), which is an important member of the heterocyclic aromatic compounds, have been widely studied in the field of pharmaceutical chemistry and other fields due to their versatile use and various biological activities.[4–8] Thiadiazole is a heterocyclic aromatic compound that has a five-member ring with 2 nitrogen atoms and one sulfur atom, in addition to carbon and hydrogen atoms. There are four different isomers of thiadiazoles named 1,2,3-thiadiazole, 1,2,4-thiadiazole, 1,2,5-thiadiazole, and 1,3,4-thiadiazole, according to the Hantzsch-Widman nomenclature.[9]

Among these isomers, 1,3,4-thiadiazole and its derivatives are especially highly reactive against many chemical reactions, and there have been many studies in the literature on the synthesis and characterization of these compounds due to their biological activities.[10–13] Heterocyclic systems in which these two bioactive compounds (imidazole and 1,3,4-thiadiazole) are fused to each other with a bridgehead nitrogen atom are referred to as imidazo[2,1-*b*][1,3,4]thiadiazoles.[14–16] These fused heterocyclic compounds and their derivatives have become widely used compounds in pharmaceutical chemistry due to their wide variety of biological activities, such as antifungal, antibacterial, antimicrobial, antioxidant, anticonvulsant, antiviral, antidepressant, anti-inflammatory, antihypertensive, antituberculosis, and antiproliferative activities.[10,17–29] Moreover, the synthesis of these compounds and their derivatives has also become a commonly investigated topic in anticancer activity studies due to their structures being similar those of Levamisole, Tetramisole, and Dexamisole, which are good immune system regulators and enhancers.[30,31]

In light of the important literature data mentioned above, this study focused on the synthesis of thioether-bridged 2,6-disubstituted imidazo[2,1-*b*][1,3,4]thiadiazole derivatives, their characterization by various spectroscopic methods, and an investigation of their antifungal activity against various plant pathogens. In addition, in silico absorption, distribution, metabolism, elimination (ADME) parameters were calculated to evaluate the drug-likeness of the synthesized compounds. Moreover, in the study, the possibility of the synthesized compounds being antifungal drug candidates was explored via docking simulations performed using the target structure *Candida albicans* sterol 14α-demethylase (CYP51) (PDB ID: 5TZ1).[32]

2 | RESULTS AND DISCUSSION

2.1 | Chemistry

In the first part of the synthesis study, 2-amino-1,-3,4-thiadiazole derivatives (**4**-**5**), the starting compounds, were obtained from the separate substitution reactions of 5-amino-1,3,4-thiadiazole-2-thiol (**3**) with 2,6-dichloro benzylbromide (**1**) and 2,6-difluorobenzylbromide (**2**) in the presence of KOH in ethyl alcohol at high yields (91% and 93%). The 2,6-dichlorobenzylbromide (**1**), 2,6-difluoro benzylbromide (**2**), and 5-amino-1,3,4-thiadiazole-2-thiol (**3**) were obtained by commercially, while the 2-amino-1,-3,4-thiadiazole derivatives (**4**-**5**) were obtained as specified in the literature.[33–36]

In the Fourier transform infrared (FTIR) spectra of the 2-amino-1,3,4-thiadiazole derivatives (**4**-**5**), symmetric and asymmetric stretching bands that corresponding to the —NH_2 group were observed as 2 separate bands at 3271 and 3074 cm^{-1}. The —C═N— group stretching bands at the thiadiazole ring were observed at 1626 and 1616 cm^{-1}.

The —NH_2 group peaks were recorded as a singlet corresponding to 2 protons at 7.42 and 7.38 ppm in the ^{1}H NMR spectra of these compounds. These peaks disappeared as a result of the proton-deuterium exchange that was performed with D_2O. The methylene protons (S-CH_2) in these compounds were observed as a singlet corresponding to 2 protons at 4.32 and 4.21 ppm, due to the electronegativity of the sulfur atom.

In the ^{13}C NMR spectra of the 2-amino-1,-3,4-thiadiazole derivatives, C_2 carbon peaks in the thiadiazole ring were observed at 147.81 and 147.62 ppm, while C_5 carbon peaks were observed at 171.76 and 171.60 ppm. In these spectra, the S-CH_2 carbons appeared at 35.99 and 27.36 ppm for compounds **4** and **5**, respectively. The ^{13}C NMR data of these compounds were highly compatible with those in the literature.[37,38]

In the second part of the synthesis study, the target compounds, thioether-bridged 2,6-disubstituted imidazo [2,1-*b*][1,3,4]thiadiazole derivatives (**7a**-**7i** and **8a**-**8i**), which contained both imidazole and thiadiazole rings, were obtained from the reactions of the starting compounds (**4** and **5**) with phenacyl bromide derivatives (**6a**-**6i**) in ethanol (at yields of 66% to 79%). The target compounds were synthesized using the synthetic pathway shown in Scheme 1.

The 2-amino-1,3,4-thiadiazole derivatives (**4** and **5**) were observed to be present in the amine-imine tautomeric form in these reactions.[1,35–37,39] In this tautomeric structure, the lone pair electron located on the —NH— in the imine form, acted as a nucleophile and was replaced by the bromine in the phenacyl bromide derivatives. The hydrogen bromide salt of the target compounds was then formed by a nucleophilic attack of the lone pair electron in the other —NH— group on phenacyl carbonyl and water separation. Finally, the target compounds were obtained by alkalinization of the medium with diluted Na_2CO_3. The proposed reaction mechanism for the formation of these compounds is shown in Scheme 2.

In the FTIR spectra of these compounds, the —NH_2 group symmetric and asymmetric absorption bands, which were found in the starting compounds (**4** and **5**) and observed in the range of 3271–3074 cm^{-1} disappeared, which was important evidence of the formation of the target compounds. Other FTIR spectral data of these compounds are given in detail in the Experimental section.

SCHEME 1 Synthetic pathways for the synthesis of thioether-bridged 2,6-disubstituted imidazo[2,1-*b*][1,3,4]thiadiazole derivatives (**7a-7i** and **8a-8i**) [Colour figure can be viewed at wileyonlinelibrary.com]

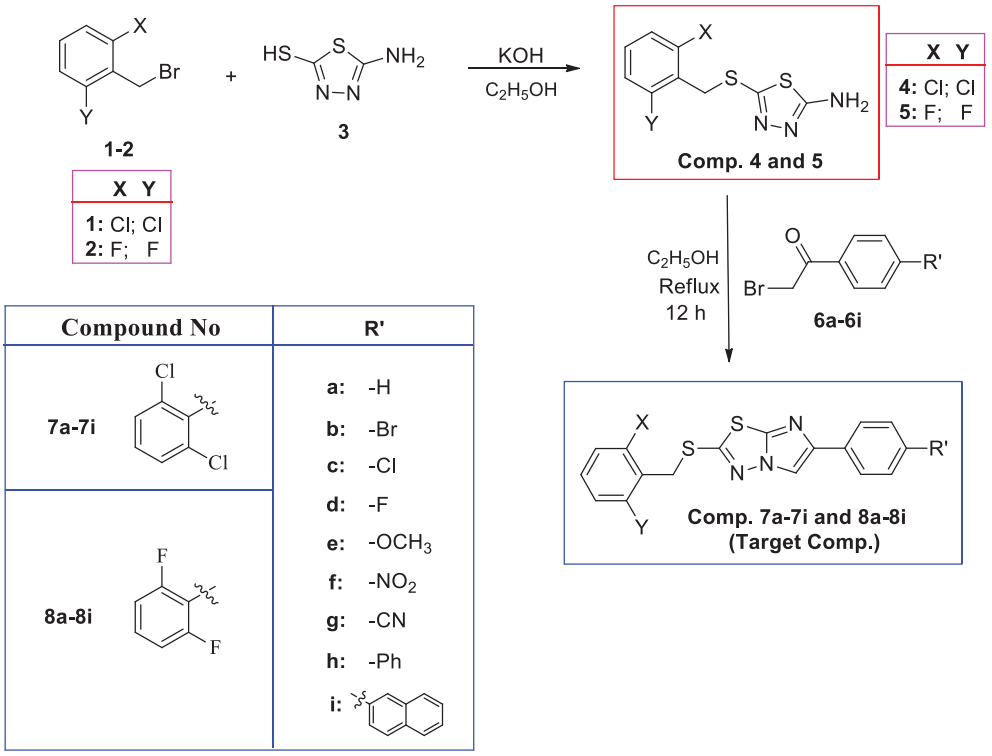

SCHEME 2 Formation mechanism of the target compounds (**7a-i** and **9a-i**) [Colour figure can be viewed at wileyonlinelibrary.com]

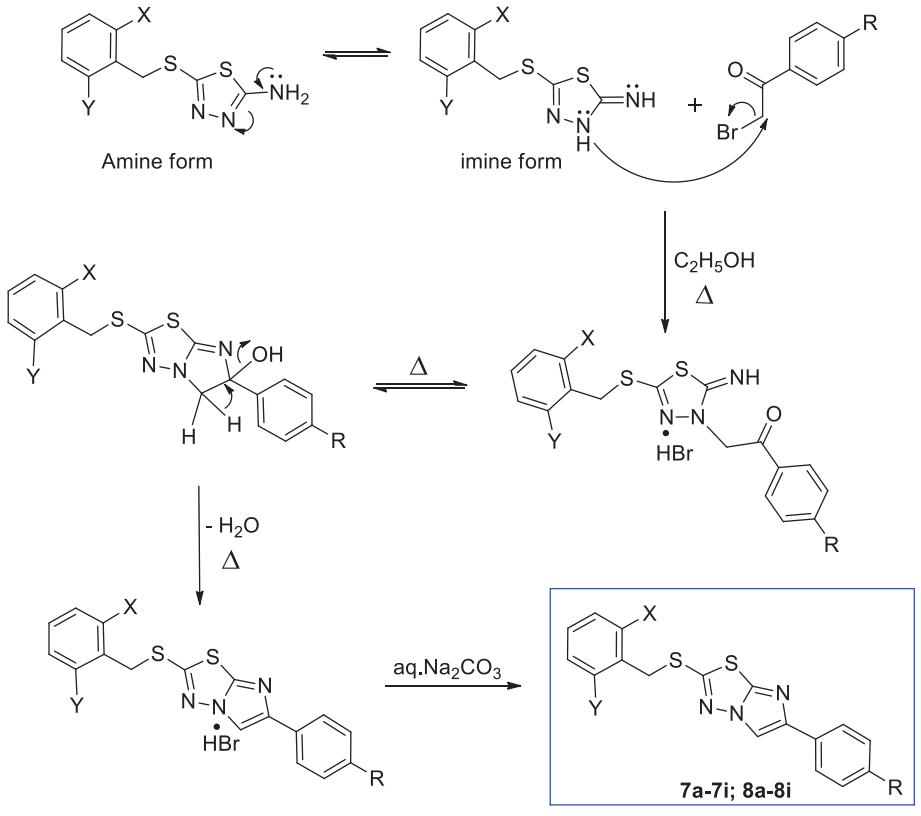

Additionally, proton signals belonging to the —NH_2 group observed at 7.42 and 7.38 ppm in the starting compounds (**4** and **5**) disappeared in the ^{1}H NMR spectra of these compounds. Instead, a 1-proton singlet that indicated C_5-H signals was observed in the range of 9.00–8.58 ppm, which was significant evidence of the formation of these compounds (**7a-7i** and **8a-8i**). This was consistent with the literature data.[1,34,39–41]

TABLE 1 Data collection and refinement values of compounds **7a**, **7d**, **8d**, **8e**, and **8g**

Molecular formula	$C_{17}H_{11}Cl_2N_3S_2$	$C_{17}H_{10}Cl_2FN_3S_2$	$C_{17}H_{10}F_3N_3S_2$	$C_{18}H_{13}F_2N_3OS_2$	$C_{18}H_{10}F_2N_4S_2$
Compounds	**7a**	**7d**	**8d**	**8e**	**8g**
Formula weight	392.31	410.30	377.40	389.43	384.42
Temperature/K	293(2)	293(2)	293(2)	293(2)	293(2)
Crystal system	triclinic	monoclinic	monoclinic	monoclinic	monoclinic
Space group	P-1	$P2_1/n$	$P2_1/c$	$P2_1/c$	$P2_1/n$
a/Å	5.5703(8)	16.783(3)	11.271(3)	12.666(3)	10.922(2)
b/Å	11.4909(18)	5.5841(7)	11.737(3)	11.391(3)	11.834(2)
c/Å	14.383(2)	19.470(3)	12.542(3)	12.618(3)	13.970(3)
α/°	69.977(5)	90	90	90	90
β/°	85.315(5)	104.995(5)	103.816(8)	107.604(7)	106.152(7)
γ/°	77.545(5)	90	90	90	90
Volume/$Å^3$	844.6(2)	1762.6(4)	1611.1(7)	1735.4(7)	1734.4(6)
Z	2	4	4	4	4
ρ_{calc} g/cm^3	1.543	1.546	1.556	1.491	1.472
μ/mm^{-1}	0.635	0.620	0.367	0.340	0.336
F(000)	400.0	832.0	768.0	800.0	784.0
Crystal size/mm^3	0.28 × 0.23 × 0.21	0.25 × 0.21 × 0.2	0.29 × 0.26 × 0.22	0.24 × 0.2 × 0.19	0.25 × 0.21 × 0.2
Radiation	MoKα (λ = 0.71073)	MoKα (λ = 0.71073)	MoKα (λ = 0.71073)	MoKα (λ = 0.71073)	MoKα (λ = 0.71073)
2Θ range for data collection/°	7.276 to 56.648	6.332 to 56.598	6.562 to 56.912	6.524 to 56.756	6.072 to 56.666
Index ranges	-7 ≤ h ≤ 7, −15 ≤ k ≤ 15, −19 ≤ l ≤ 19	−22 ≤ h ≤ 22, −7 ≤ k ≤ 7, −25 ≤ l ≤ 25	−15 ≤ h ≤ 13, −15 ≤ k ≤ 15, −16 ≤ l ≤ 16	−16 ≤ h ≤ 16, −15 ≤ k ≤ 15, −16 ≤ l ≤ 14	−14 ≤ h ≤ 14, −15 ≤ k ≤ 15, −18 ≤ l ≤ 18
Reflections collected	31,776	60,083	31,268	53,903	44,895
Independent reflections	3834 [R_{int} = 0.0293, R_{sigma} = 0.0198]	4378 [R_{int} = 0.0480, R_{sigma} = 0.0215]	3826 [R_{int} = 0.0613, R_{sigma} = 0.0359]	4129 [R_{int} = 0.0436, R_{sigma} = 0.0268]	4135 [R_{int} = 0.0379, R_{sigma} = 0.0248]
Data/restraints/parameters	3834/0/218	4378/0/227	3826/0/227	4129/0/237	4135/0/236
Goodness-of-fit on F^2	1.111	1.075	1.098	1.086	1.100
Final R indexes [I > =2σ (I)]	R_1 = 0.0439, wR_2 = 0.0802	R_1 = 0.0558, wR_2 = 0.1197	R_1 = 0.0635, wR_2 = 0.1272	R_1 = 0.0626, wR_2 = 0.1070	R_1 = 0.0864, wR_2 = 0.1506
Final R indexes [all data]	R_1 = 0.0535, wR_2 = 0.0870	R_1 = 0.0669, wR_2 = 0.1280	R_1 = 0.0783, wR_2 = 0.1393	R_1 = 0.0895, wR_2 = 0.1228	R_1 = 0.1067, wR_2 = 0.1627
Largest diff. peak/hole/e $Å^{-3}$	0.28/−0.30	0.46/−0.38	0.33/−0.41	0.27/−0.30	0.36/−0.36

TABLE 1 (Continued)

Molecular formula	$C_{17}H_{11}Cl_2N_3S_2$	$C_{17}H_{10}Cl_2FN_3S_2$	$C_{17}H_{10}F_3N_3S_2$	$C_{18}H_{13}F_2N_3OS_2$	$C_{18}H_{10}F_2N_4S_2$
CCDC Deposition Number	2,050,752	2,050,753	2,050,751	2,050,754	2,050,755

Signals that appeared in the range of 113.87 to 109.83 and 146.37 to 143.29 ppm in the ^{13}C NMR spectrum of these compounds were important evidence of ring cyclization. These signals corresponded to the C_5 and C_6 carbons of the imidazo[2,1-*b*][1,3,4]thiadiazole derivatives (**7a**-**7i** and **8a**-**8i**). Also, in ^{13}C NMR spectra of fluorine containing compounds **5**, **7d**, and **8a-8i** splitting were observed due to quite distinct C-F couplings. In coupling constants, it was observed that especially the coupling in the ^{1}J CF position was severe and splitting occurred corresponding to approximately 239 to 254 Hz range. ^{13}C NMR carbon data of the compounds, which were highly consistent with the literature, can be found in the Experimental part of this study, in detail.[1,35–37]

Additionally, the mass spectra of all of the synthesized compounds in the study were observed as expected and were supported by the molecular ion peaks. The spectroscopic data for all of the synthesized compounds are given in detail in Experimental section and the relevant spectra are given in Supplementary Material section.

Finally, single crystals of compounds **7a**, **7d**, **8d**, **8e**, and **8g** were obtained and their structures were confirmed by X-ray analysis. The crystallographic data and crystal structures and of these compounds are shown in Table 1 and Figure 1, respectively. Bond lengths, bond angles, and packing structures of compounds **7a**, **7d**, **8d**, **8e**, and **8g** are given in Supplementary Material section.

2.2 | In vitro antifungal activity and structure-activity relationship studies

In the *in vitro* antifungal activity studies, mycelial growth, mycelial growth inhibition, minimum inhibitory concentration (MIC), minimum fungicidal activity (MFC), and lethal dose (LD_{50}) values against the tested fungus species were determined for all of the compounds synthesized in the study. Varying rates of activity were observed with all of the doses of the compounds used, depending on the type of fungi. The activity increased as the dose increased. The type of pathogen that had the highest sensitivity to the compounds was *A. solani*; Followed by *F. oxysporum f. sp. melonis* and *V. dahliae*. Mycelial growth inhibition (MGI) rates (Figure 2) of doses of 8 and 20 μg/mL, which showed the highest activity, were calculated in the mycelial growth activity studies of the fungus species (Table 2). Looking at the activity results of all of the compounds, the mycelial growth inhibition was 11% to 93% for *A. solani*, 21% to 58% for *V. dahliae*, and 13% to 73% for *F. oxysporum f.sp. melonis*. Thiram (80%), used in the positive control, inhibited mycelium growth of all of the fungi by 100%. Dimethyl sulfoxide (DMSO), used as negative control, did not inhibit mycelium growth of the fungi, as expected. The LD_{50}, MFC, and MIC values of the compounds against the fungi were calculated as well (Table 3). The highest and lowest LD_{50} values against the plant pathogens were 79.3 and 7.3 μg/mL against *A. solani*, 104.1 and 12.6 μg/mL against *F. oxysporum f.sp. melonis*, and 91.4 and 14.3 μg/mL against *V. dahliae*. The MFC values ranged from >10 to >40 μg/mL. Similarly, the MIC values varied between 0.625 and 2.5 μg/mL, depending on the reaction of each fungus species against the compounds (Table 3). According to all of the test results, the compounds were found to have moderate to high levels of antifungal activity against the fungus species.

Antifungal activity of the compounds against the plant pathogen fungi tested in the study were observed to be at different levels for each compound. Compounds with 50% or higher (moderate and high levels) activity against the pathogens in order of effectiveness were **7b**, **7c, 7d**, **7e**, **7f**, **8a, 8d**, **8i**, and **7i** for *Alternaria solani*; **7a**, **7b**, **7c**, **7e, 7i**, and **8d** for *Fusarium oxysporum f.sp. melonis*; and **4**, **7e**, and **8c** for *Verticillium dahliae*. Compound **7e** showed moderate to good antifungal activity against all of the plant pathogens.

Furthermore, a structure-activity relationship (SAR) study was conducted on the target compounds. The primary aim in the SAR study was the modification of the aromatic ring shown as the X and Y groups. The 2,6-dichlorobenzyl and 2,6-difluorobenzyl groups were used to achieve this. The antifungal activity results (Tables 2 and 3, Figure 2) generally showed a higher level of activity in compounds **7a-7i** with the 2,6-dichlorophenyl group as the R group when compared to compounds **8a-8i** with the 2,6-difluorobenzyl group. The secondary aim was to change the substitute groups on the phenyl ring displayed as R′. Electron donating

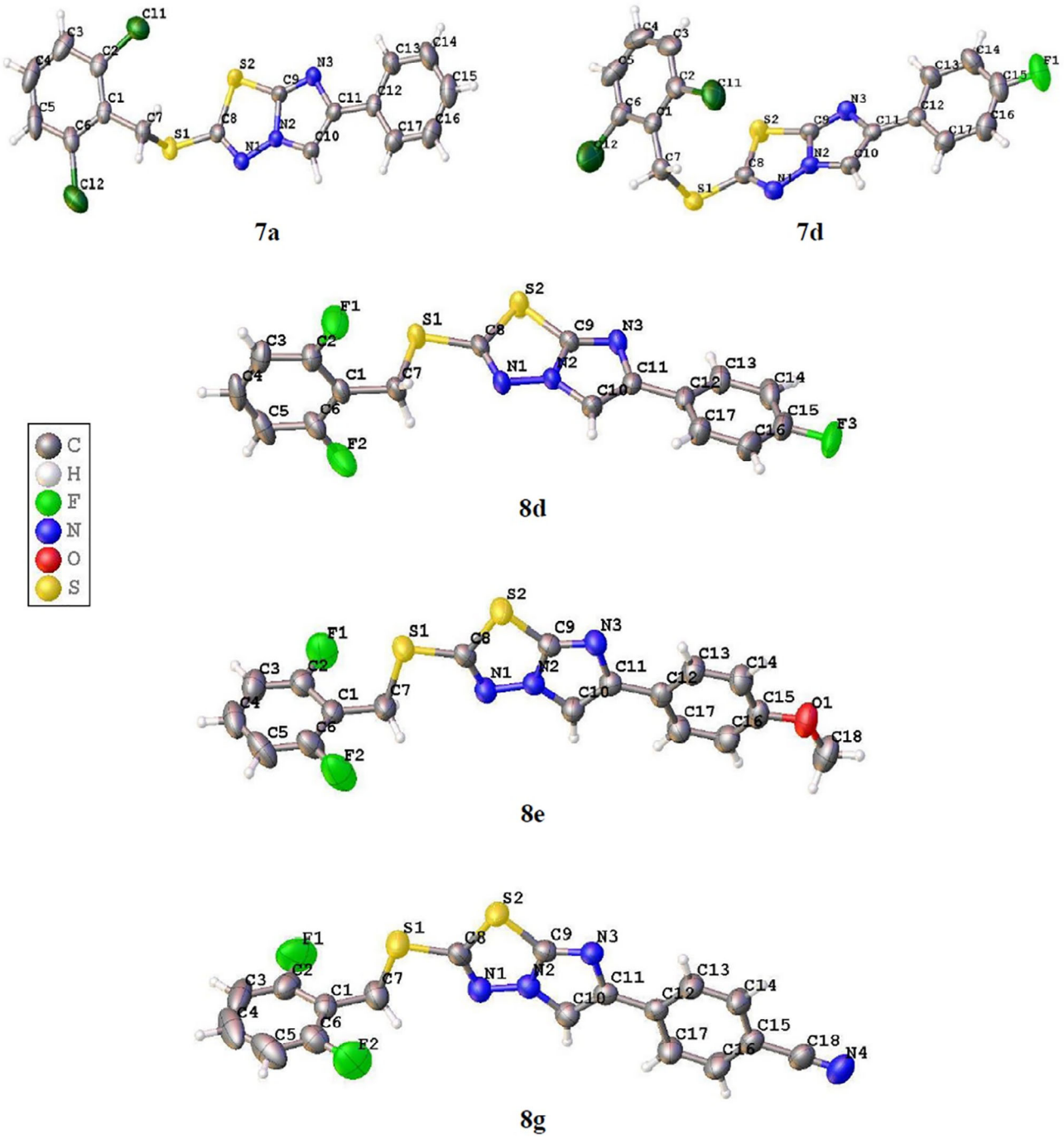

FIGURE 1 Crystal structures of compounds **7a**, **7d**, **8d**, **8e**, and **9g** [Colour figure can be viewed at wileyonlinelibrary.com]

groups such as methoxy, phenyl, and naphthyl; electron-withdrawing groups, such as bromo, chloro, fluoro, cyano, and nitro groups were chosen as the substituents and the R′ groups to confer the effect of different electronic environments on the activities. In this case, the antifungal activity of all of the synthesized compounds was quite different, but their structures were similar; therefore, the activity was related to the influence of the different groups on the phenyl ring with different steric and electronic effects. In the SAR study, the presence of electron-withdrawing groups, such as —Br, Cl, and —F, linked to the four positions of the phenyl ring in compounds **7b, 7c, 7d**, and **8d**, displayed high activity against *Alternaria solani*. Activity was observed to decrease when the steric effect was increased in electron donor groups (phenyl and naphthyl) that are linked to the phenyl ring in compounds **7h** and **8h**. As seen in Tables 2 and 3, the presence of electron-withdrawing groups (-Br and -Cl)

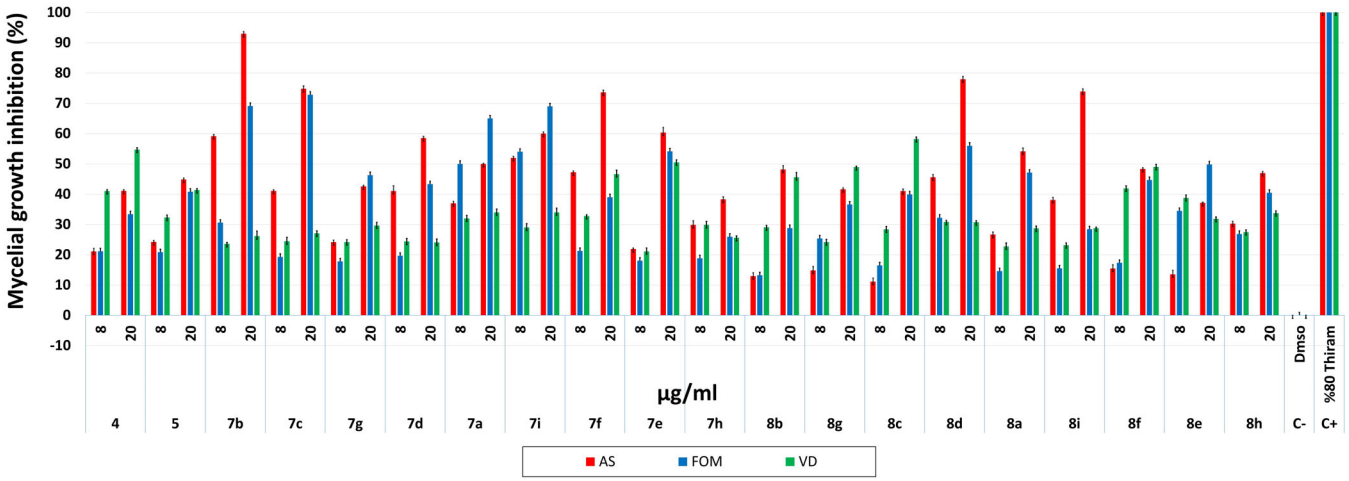

FIGURE 2 Mycelial growth inhibition of the compounds against *A. solani* (AS), *F. oxysporum f. sp. melonis* (FOM), and *V. dahliae* (VD) for doses of 8 and 20 µg/mL. C+: Thiram (positive control). C−: DMSO (negative control) [Colour figure can be viewed at wileyonlinelibrary.com]

increased the antifungal activity against *Fusarium oxysporum f.sp.melonis* in compounds **7b** and **7c**. In contrast, activity was observed to decrease dramatically with the increase of the steric effect against *Fusarium oxysporum f.sp.melonis* in compounds **7h** and **8i**. Moreover, in compound **8g**, the presence of the electron-withdrawing -CN group showed the highest level of activity against *Vertcillium dahlia*.

The SAR study revealed that the presence of electron-withdrawing groups and less bulky groups had significant effects on the antifungal activity in generally. These results were also consistent with the literature.[1,35–37,42]

2.3 | In Silico ADME and molecular docking studies

Insufficient evaluation of the ADME parameters causes many biologically active compounds to fail to reach the level for clinical use. For this reason, it is of great importance to evaluate the ADME parameters of newly synthesized drug candidate compounds and their similarity to existing drugs. In this context, the ADME parameters of all of the synthesized compounds were calculated first. Table 4 shows the resulting values.

The physicochemical parameters calculated in the study included the molecular weight (MW), heavy atom count, fraction of sp^3 carbon atoms (Fsp^3), various bond properties, molar refraction (MR), and topological polar surface area (tPSA). Among these, the MR value is defined as a measure of the overall polarity of a molecule, and this parameter, used by the Ghose filter [43], is usually expected to be in the range of 40 to 130. Looking at Table 4, it can be seen that all of the synthesized compounds were in this recommended range. The tPSA, on the other hand, is the sum of the surface areas of polar atoms in a molecule and is a parameter related to the drug-carrying capacity of a molecule. According to Table 4, it was observed that the values obtained for the synthesized compounds provided the values recommended by various drug filters (≤131.6 for Egan[44], ≤140 for Veber[45], ≤157 for Muegge[46]). On the other hand, the Fsp^3 is an index that shows drug likeness and has only recently been introduced.[47,48] Lovering et al conducted a study in the 0.1 to 0.9 Fsp^3 value range, and reported that an increasing Fsp^3 value led to decreased cytochrome (CYP) inhibition.[49] In other words, the low Fsp^3 value of a molecule suggests that it may have a significant inhibitory effect on CYP enzymes. As can be seen in Table 4, the very low values of the compounds indicated that these newly synthesized compounds were quite likely to be CYP inhibitors. In addition, the lipophilicity parameters shown in Table 4 referred to the ability of the chemical compounds to dissolve in fats, lipids, and apolar solvents, such as hexane or toluene, and was therefore an important parameter that affects the activity of the drug in the human body. The LogP value is the most commonly used measure of lipophilicity and is an indicator of the permeability of drugs to reach the target tissue in the body. In this context, the LogP values used by the major drug filters and their mean values (consensus LogP) are shown in Table 4.

Most of the ADME parameters and lipophilicity criteria that are calculated and shown in Table 4 were the basic metrics used by major drug filter approaches. Five major drug filters, including Lipinski[50] (Pfizer), Ghose, Veber (GSK), Egan (Pharmacia), and Muegge (Bayer), were used in this study to evaluate the drug-likeness of the synthesized compounds. Table 5 shows the criteria for

TABLE 2 Mycelial growth of the compounds against plant pathogenic fungi

	Mycelial growth (mm)[a]																	
	Alternaria solani						*Fusarium oxysporum f. sp. melonis*						*Verticillium dahliae*					
	Doses (μg/mL)						Doses (μg/mL)						Doses (μg/mL)					
Compounds	**0.5**	**1**	**2**	**4**	**8**	**20**	**0.5**	**1**	**2**	**4**	**8**	**20**	**0.5**	**1**	**2**	**4**	**8**	**20**
4	60 ± 0.0	59 ± 1.9	55 ± 0.6	53 ± 0.4	47 ± 1.0	35 ± 1.1	54 ± 1.7	55 ± 0.4	54 ± 1.5	52 ± 1.7	47 ± 1.3	40 ± 1.4	58 ± 0.7	48 ± 0.8	44 ± 2.2	46 ± 1.5	35 ± 2.9	27 ± 2.0
5	59 ± 1.2	59 ± 1.1	54 ± 1.3	53 ± 0.9	45 ± 2.3	33 ± 0.6	60 ± 0.0	56 ± 0.2	52 ± 0.5	50 ± 0.9	47 ± 1.6	36 ± 4.1	59 ± 0.4	58 ± 1.6	47 ± 0.9	45 ± 0.6	41 ± 2.5	35 ± 2.1
7a	60 ± 0.0	56 ± 0.5	55 ± 1.0	49 ± 0.1	38 ± 0.6	30 ± 0.1	55 ± 0.1	47 ± 0.8	41 ± 0.6	34 ± 0.1	30 ± 0.4	21 ± 0.8	59 ± 0.2	47 ± 0.4	45 ± 0.3	44 ± 0.5	41 ± 0.4	40 ± 0.7
7b	60 ± 0.0	60 ± 0.0	55 ± 0.9	54 ± 0.6	24 ± 0.4	4 ± 0.9	60 ± 0.0	58 ± 3.0	54 ± 1.0	52 ± 0.5	42 ± 0.4	19 ± 3.8	49 ± 0.7	48 ± 1.8	49 ± 2.3	47 ± 0.8	46 ± 2.1	44 ± 2.8
7c	60 ± 0.0	52 ± 0.7	50 ± 0.7	43 ± 0.5	35 ± 1.3	15 ± 1.1	55 ± 0.9	55 ± 0.9	53 ± 0.8	50 ± 0.4	48 ± 1.6	16 ± 2.2	49 ± 0.9	47 ± 1.0	48 ± 5.0	48 ± 0.8	45 ± 1.3	44 ± 1.5
7d	60 ± 0.0	60 ± 0.0	55 ± 1.4	44 ± 0.4	35 ± 2.3	25 ± 3.0	60 ± 0.0	57 ± 3.3	54 ± 0.2	51 ± 0.9	48 ± 1.6	34 ± 3.0	49 ± 0.9	49 ± 1.3	47 ± 0.9	47 ± 0.7	45 ± 2.3	46 ± 1.4
7e	60 ± 0.0	55 ± 0.5	52 ± 0.4	51 ± 0.7	47 ± 1.5	24 ± 1.2	60 ± 0.0	55 ± 0.3	55 ± 1.0	51 ± 1.3	49 ± 0.8	28 ± 2.0	59 ± 0.6	58 ± 0.7	48 ± 1.3	47 ± 0.5	47 ± 2.9	30 ± 3.2
7f	60 ± 0.0	52 ± 0.9	52 ± 0.6	51 ± 1.2	32 ± 0.1	16 ± 2.0	60 ± 0.0	60 ± 0.0	54 ± 0.4	53 ± 0.4	47 ± 1.4	37 ± 0.9	59 ± 0.4	57 ± 0.7	55 ± 0.3	46 ± 0.6	40 ± 2.2	32 ± 2.8
7g	60 ± 0.0	56 ± 0.1	55 ± 0.3	53 ± 1.0	46 ± 1.1	34 ± 3.8	59 ± 1.3	54 ± 0.3	52 ± 1.1	51 ± 0.9	49 ± 1.7	32 ± 3.3	46 ± 1.5	48 ± 1.9	46 ± 0.6	47 ± 0.4	46 ± 1.1	42 ± 0.9
7h	60 ± 0.0	59 ± 0.7	56 ± 0.8	54 ± 0.2	42 ± 1.5	37 ± 1.7	54 ± 2.3	55 ± 0.6	55 ± 0.3	53 ± 0.7	49 ± 26	44 ± 1.6	49 ± 0.8	48 ± 0.7	48 ± 1.3	47 ± 0.5	42 ± 1.5	45 ± 1.3
7i	59 ± 0.0	54 ± 0.1	52 ± 0.5	46 ± 0.9	29 ± 0.3	24 ± 0.8	54 ± 0.3	52 ± 0.7	49 ± 0.5	40 ± 0.4	27 ± 0.5	19 ± 0.7	59 ± 0.4	46 ± 0.1	46 ± 0.2	43 ± 0.9	43 ± 1.0	39 ± 0.1
8a	60 ± 0.0	53 ± 1.1	55 ± 0.8	53 ± 0.8	44 ± 0.5	27 ± 1.3	59 ± 1.1	59 ± 1.8	55 ± 1.9	53 ± 0.9	51 ± 1.1	32 ± 1.3	48 ± 1.3	50 ± 0.7	50 ± 1.7	49 ± 1.0	46 ± 2.3	43 ± 1.5
8b	60 ± 0.0	60 ± 0.0	58 ± 2.0	53 ± 0.3	52 ± 0.2	31 ± 1.8	60 ± 0.0	60 ± 0.0	55 ± 0.8	54 ± 0.4	52 ± 0.8	43 ± 2.7	60 ± 0.6	48 ± 0.3	47 ± 1.6	47 ± 0.6	43 ± 0.9	33 ± 2.0
8c	55 ± 0.6	56 ± 1.2	54 ± 0.4	54 ± 0.5	51 ± 0.7	35 ± 3.1	60 ± 0.0	58 ± 3.8	55 ± 0.5	54 ± 0.4	45 ± 1.8	38 ± 2.2	59 ± 1.2	58 ± 0.6	49 ± 0.9	47 ± 2.0	45 ± 0.8	31 ± 3.8
8d	60 ± 0.1	55 ± 0.3	54 ± 0.3	44 ± 0.6	33 ± 1.4	13 ± 2.4	60 ± 0.0	60 ± 0.0	55 ± 1.5	51 ± 0.8	41 ± 1.4	26 ± 2.3	46 ± 4.0	47 ± 2.1	49 ± 0.2	47 ± 0.7	41 ± 0.9	42 ± 1.6
8e	60 ± 0.0	60 ± 0.0	60 ± 0.0	54 ± 0.4	52 ± 1.0	38 ± 2.1	60 ± 0.0	60 ± 0.1	55 ± 0.2	52 ± 1.2	39 ± 2.8	30 ± 2.4	49 ± 1.3	50 ± 1.1	47 ± 0.8	47 ± 0.4	37 ± 5.8	41 ± 0.3
8f	59 ± 2.2	56 ± 1.1	54 ± 0.1	54 ± 0.6	51 ± 0.9	31 ± 1.9	59 ± 1.3	57 ± 1.3	55 ± 0.4	52 ± 1.5	50 ± 2.6	33 ± 2.1	50 ± 0.7	49 ± 0.7	49 ± 1.1	47 ± 1.1	35 ± 1.5	31 ± 1.1
8g	53 ± 2.3	55 ± 0.7	55 ± 0.8	54 ± 0.5	53 ± 0.6	35 ± 5.2	60 ± 0.0	57 ± 1.4	54 ± 0.2	52 ± 1.1	50 ± 1.8	36 ± 3.0	60 ± 0.4	59 ± 0.7	49 ± 1.4	44 ± 2.1	43 ± 2.1	25 ± 1.6
8h	60 ± 0.0	60 ± 0.0	55 ± 0.4	53 ± 0.4	42 ± 2.0	32 ± 2.7	59 ± 1.2	56 ± 0.4	54 ± 0.5	51 ± 1.4	44 ± 2.5	36 ± 0.5	49 ± 0.6	48 ± 0.7	49 ± 0.3	47 ± 1.4	44 ± 1.1	40 ± 2.8
8i	60 ± 0.0	60 ± 0.5	53 ± 0.5	52 ± 3.1	37 ± 4.4	16 ± 1.6	58 ± 1.5	55 ± 0.3	55 ± 0.4	54 ± 0.7	51 ± 0.7	43 ± 3.7	48 ± 0.5	49 ± 1.8	49 ± 1.2	50 ± 1.1	46 ± 0.7	43 ± 1.3
C−	60 ± 0.0	60 ± 0.0	60 ± 0.0	60 ± 0.0	60 ± 0.0	60 ± 0.0	60 ± 0.0	60 ± 0.0	60 ± 0.0	60 ± 0.0	60 ± 0.0	60 ± 0.0	60 ± 0.0	60 ± 0.0	60 ± 0.0	60 ± 0.0	60 ± 0.0	60 ± 0.0
C+	0 ± 0.0	0 ± 0.0	0 ± 0.0	0 ± 0.0	0 ± 0.0	0 ± 0.0	0 ± 0.0	0 ± 0.0	0 ± 0.0	0 ± 0.0	0 ± 0.0	0 ± 0.0	0 ± 0.0	0 ± 0.0	0 ± 0.0	0 ± 0.0	0 ± 0.0	0 ± 0,0

Note: Mycelial growth (MG) ± standard deviation (SD). C+: Positive control (Thiram). C−: Negative control (DMSO).

[a]Mean of the three assays.

TABLE 3 Antifungal activity values (LD_{50}, MIC, and MFC) of the compounds against the phytopathogenic fungi

	(LD_{50}[a]/MIC[b]/MFC[c] μg/mL)		
Compounds	***Alternaria solani***	***Fusarium oxysporum f.sp.melonis***	***Verticillium dahliae***
4	28.7/<1.25/<40	80.3/0.625/>40	14.3/<0.625/20
5	26.1/<1.25/<40	27.9/<1.25/>40	23.5/<0.625/>20
7a	27.9/1.25/>40	14,9/>1.25/>20	24.9/ <0.625/>40
7b	7.3/1.25/10	12.6/>1.25/>20	77.5/ <0.625/>40
7c	8.6/<2.5/>10	15.2/>0.625/>20	26.8/ <0.625/<40
7d	12.2/<2,5/>20	23.4/<2.5/>40	91.4/ <0.625/>40
7e	17.2/<0.625/>20	16.1/>0.625/>20	20.4/<0.625/>20
7f	9.5/<0.625/20	22.5/>1.25/>40	20.1/<0.625/>20
7g	26.1/1.25/>40	23.1/<1.25/>40	31.2/ <0.625/>20
7h	20.8/<1.25/>20	104.1/>0.625/>40	61.2/ <0.625/>40
7i	16.2/1.25/>20	15.2/>0.625/>20	48.9/ <0.625/<40
8a	19.1/0.625/ >20	21.9/>0.625/>40	91.1/ <0.625/>40
8b	23.5/<2.5/ >40	37.1/<2.5/>40	25.7/<1.25/>20
8c	71.2/1.25/>40	41.4/1.25/>40	21.5/<0.625/>20
8d	8.5/>1.25/>10	15.3/>2.5/>20	32.5/<0.625/>20
8e	29.5/<5/>40	17.3/1.25/>20	15.1/ <0.625/20
8f	27.4/<2.5/>40	25.6/>0.625/>40	26.8/ <0.625/>20
8g	79.3/<2.5/>40	26.5/<1.25/>40	14.7/<1.25/>20
8h	19.5/<1.25/40	31.5/>0.625/>40	46.4/ <0.625/40
8i	10.1/<1.25/20	62.8/>0.625/>40	76.6/ <0.625/>40
C+	11.9/>0.625/<3000	11.3/>0.625/<3000	14.34/<1.25/<3000

Note: C+: Positive control (Thiram 80%).
[a]LD_{50}: The amount of a compound, which causes the death of 50% (one half) of test fungi.
[b]MIC: Minimum inhibitory concentration.
[c]MFC: Minimum fungicidal concentration.

these drug-likeness filters, the criteria violation numbers of synthesized compounds, and the parameters that were violated. Looking at Table 5, it can be seen that compounds **4g**, **5g**, and **8g** fully met the criteria of all of the filters and did not violate any criteria. In addition, all of the compounds meet the criteria of the Veber filter. Considering compounds other than **4g**, **5g**, and **8g** for the other four filters, **8f** violated the Ghose filter once, **7g** and **8e** violated the Ghose and Muegge filters once, and **7f** and **8a** violated the Lipinski, Ghose, and Muegge filters once. Compounds other than these violated these four filters once. In addition, all of the mentioned violations were related to the lipophilicity parameters of the compounds. As is known, filtering approaches mostly state that an orally active drug should not violate the criteria more than once. In this context, it can be said that all of the synthesized compounds generally met the filtration conditions.

On the other hand, the Fsp^3 values in Table 4 indicated that the synthesized compounds could be CYP inhibitors. In this context, the possibility of the synthesized compounds being antifungal drug candidates was explored via molecular docking studies on the target structure, *Candida albicans* sterol 14α-demethylase (CYP51) (PDB ID: 5TZ1), of a CYPP450 enzyme. The main reason that the 5TZ1 CYP structure was selected was that the inhibitory effect for the most commonly used antifungal drugs was studied on this structure and then they were compared with each other.[32] The results of the relevant study reported that posaconazole and VT-1161 were shown to be the most potent inhibitors of 5TZ1. In this context, comparing the results of the docking simulations with these potent inhibitors was of great importance for evaluating the potential of the synthesized compounds as possible antifungal drugs. Table 5 shows the highest binding energy values found as a result of the molecular docking simulations performed for the synthesized compounds and these two potent inhibitors on the 5TZ1 target structure. The results showed that all of the synthesized compounds, except compounds **4** and **5**, gave

TABLE 4 Various ADME properties of all of the compounds

	Physicochemical properties									Lipophilicity					
Compounds	MW (g/mol)	Heavy atoms	Aromatic heavy atoms	Fsp^3	RB	HBA	HBD	MR	tPSA ($Å^2$)	ilogP	XlogP	WlogP	MlogP	SILICOS-IT	Consensus logP
4	292.21	16	11	0.11	3	2	1	70.54	105.34	2.48	3.61	3.58	2.66	4.10	3.29
5	259.30	16	11	0.11	3	4	1	60.44	105.34	1.95	2.56	3.39	2.36	3.66	2.78
7a	392.33	24	20	0.06	4	2	0	102.53	83.73	3.66	6.10	5.91	4.57	5.77	5.20
7b	471.22	25	20	0.06	4	2	0	110.23	83.73	4.12	6.79	6.67	5.18	6.45	5.84
7c	426.77	25	20	0.06	4	2	0	107.54	83.73	4.02	6.73	6.56	5.07	6.41	5.76
7d	410.32	25	20	0.06	4	3	0	102.49	83.73	3.91	6.20	6.46	4.96	6.19	5.54
7e	422.35	26	20	0.11	5	3	0	109.02	92.96	4.02	6.07	5.91	4.22	5.81	5.21
7f	437.32	27	20	0.06	5	4	0	111.35	129.55	3.19	5.93	5.81	4.38	3.60	4.58
7g	417.33	26	20	0.06	4	3	0	107.24	107.52	3.79	5.82	5.78	3.88	5.79	5.01
7h	468.42	30	26	0.04	5	2	0	127.96	83.73	4.34	7.73	7.57	5.67	7.30	6.52
7i	442.38	28	24	0.05	4	2	0	120.03	83.73	4.12	7.35	7.06	5.28	6.77	6.12
8a	359.42	24	20	0.06	4	4	0	92.42	83.73	3.45	5.05	5.72	4.34	5.34	4.78
8b	438.31	25	20	0.06	4	4	0	100.12	83.73	3.84	5.74	6.48	4.96	6.01	5.40
8c	393.86	25	20	0.06	4	4	0	97.43	83.73	3.73	5.68	6.37	4.84	5.97	5.32
8d	377.41	25	20	0.06	4	5	0	92.38	83.73	3.56	5.15	6.28	4.73	5.75	5.09
8e	389.44	26	20	0.11	5	5	0	98.92	92.96	3.77	5.02	5.73	3.99	5.37	4.78
8f	404.41	27	20	0.06	5	6	0	101.25	129.55	2.90	4.88	5.63	4.14	3.16	4.14
8g	384.43	26	20	0.06	4	5	0	97.14	107.52	3.45	4.77	5.59	3.65	5.35	4.56
8h	435.51	30	26	0.04	5	4	0	117.86	83.73	4.14	6.67	7.38	5.46	6.86	6.10
8i	409.47	28	24	0.05	4	4	0	109.93	83.73	3.83	6.30	6.87	5.07	6.33	5.68

Abbreviations: HBA, hydrogen bond acceptor; HBD, hydrogen bond donor; RB, rotatable bonds.

TABLE 5 Drug-likeness, skin permeation, water-solubility properties, and docking scores of all of the compounds

	Violation of drug-likeness filters					Skin permeation	Water solubility		Docking
Comp.	**Lipinski**	**Ghose**	**Veber**	**Egan**	**Muegge**	**Log K_p (cm/s)**	**ESOL**	**Class**	**Binding energy**
	MW≤500 MlogP ≤4.15 HBA≤10 HBD≤5	160 ≤ MW≤480 0.4 ≤ WlogP≤5 40 ≤ MR≤130 20 ≤ atoms≤70	RB≤10 TPSA≤140	WlogP≤5.88 TPSA≤131.6	200 ≤ MW≤600– 2 ≤ XLOGP≤5 TPSA≤157 HBA≤10 HBD≤5 RB ≤15 Rings≤7 Carbons>4 Heteroatoms>1				
4	0	0	0	0	0	−5.52	−4.24	Moderately	−7.1
5	0	0	0	0	0	−6.06	−3.37	Soluble	−7.2
7a	1: MlogP>4.15	1: WlogP>5.6	0	1: WlogP>5.88	1: XlogP>5	−4.36	−6.47	Poorly	−10.1
7b	1: MlogP>4.15	1: WlogP>5.6	0	1: WlogP>5.88	1: XlogP>5	−4.35	−7.37	Poorly	−9.6
7c	1: MlogP>4.15	1: WlogP>5.6	0	1: WlogP>5.88	1: XlogP>5	−4.12	−7.05	Poorly	−9.6
7d	1: MlogP>4.15	1: WlogP>5.6	0	1: WlogP>5.88	1: XlogP>5	−4.40	−6.62	Poorly	−10.2
7e	1: MlogP>4.15	1: WlogP>5.6	0	1: WlogP>5.88	1: XlogP>5	−4.57	−6.52	Poorly	−9.9
7f	1: MlogP>4.15	1: WlogP>5.6	0	0	1: XlogP>5	−4.76	−6.51	Poorly	−9.7
7g	0	1: WlogP>5.6	0	0	1: XlogP>5	−4.71	−6.40	Poorly	−10.0
7h	1: MlogP>4.15	1: WlogP>5.6	0	1: WlogP>5.88	1: XlogP>5	−3.67	−7.93	Poorly	−11.5
7i	1: MlogP>4.15	1: WlogP>5.6	0	1: WlogP>5.88	1: XlogP>5	−3.78	−7.58	Poorly	−11.0
8a	1: MlogP>4.15	1: WlogP>5.6	0	0	1: XlogP>5	−4.91	−5.60	Moderately	−10.1
8b	1: MlogP>4.15	1: WlogP>5.6	0	1: WlogP>5.88	1: XlogP>5	−4.90	−6.50	Poorly	−9.8
8c	1: MlogP>4.15	1: WlogP>5.6	0	1: WlogP>5.88	1: XlogP>5	−4.67	−6.19	Poorly	−9.8
8d	1: MlogP>4.15	1: WlogP>5.6	0	1: WlogP>5.88	1: XlogP>5	−4.95	−5.75	Moderately	−10.0
8e	0	1: WlogP>5.6	0	0	1: XlogP>5	−5.11	−5.66	Moderately	−9.7
8f	0	1: WlogP>5.6	0	0	0	−5.30	−5.64	Moderately	−9.7
8g	0	0	0	0	0	−5.26	−5.53	Moderately	−10.0
8h	1: MlogP>4.15	1: WlogP>5.6	0	1: WlogP>5.88	1: XlogP>5	−4.22	−7.05	Poorly	−11.7
8i	1: MlogP>4.15	1: WlogP>5.6	0	1: WlogP>5.88	1: XlogP>5	−4.32	−6.72	Poorly	−11.2

values close to the potent inhibitors of the target structure, posaconazole (−11.8 kcal/mol) and VT-1161 (−11.3 kcal/mol). Compounds **7h** (−11.5 kcal/mol), **7i** (−11.0 kcal/mol), **8h** (−11.7 kcal/mol) and **8i** (−11.2 kcal/mol), in particular, can be said to have as much potential as these potent inhibitors. Additionally, examining the binding regions of the compounds in 3D, it can be said that all of the compounds synthesized in the study, posaconazole, and VT-1161 bound to the 5TZ1 target structure from approximately the same region, and they all had very similar conformational orientation (Figure 3). In order to further deepen the study, Table 6 shows the residues of 5TZ1 interacting with the relevant molecules and the interactions types. Looking at Table 6, the hydrophobic interactions appeared to be more dominant for all of the compounds. In addition, considering the hydrogen bonds, which directly affect the drug properties of molecules, all of the molecules, except compound **8h** and posaconazole, had at least one hydrogen bond interaction with 5TZ1. Moreover, posaconazole appeared to have no electrostatic interaction at all. Moreover, all of the other molecules, except VT-1161, seemed to have at least one PiSu (Pi-Sulfur) interaction with 5TZ1. Figures 4 to 9 show the 2D interaction diagrams, to provide a better understanding of the binding regions of the compounds with the highest binding affinity to 5TZ1 (**7h**, **7i**, **8h**, and **8i**), and the most potent inhibitors of 5TZ1, posaconazole and VT-1161, to the target structure.

3 | CONCLUSION

In conclusion, thioether-bridged 2,6-disubstituted imidazo[2,1-*b*][1,3,4]thiadiazole derivatives were synthesized under simple and mild reaction conditions. The structure of the synthesized compounds was characterized using spectroscopic analysis techniques.

Mycelial growth, mycelial growth inhibition, and MIC, MFC and LD_{50} values against various plant pathogenic fungi were determined for all of the target compounds through *in vitro* antifungal activity tests. The results of the tests showed that compounds **7b**, **7c**, **7d, 7f**, **8d** and **8g** had good antifungal activity against the plant pathogens.

In addition, as a result of the in silico ADME assessments, all of the compounds synthesized in the study can be said to have generally met the rules of the five major drug-likeness filters. Finally, docking simulations on the 5TZ1 target structure showed that compounds **7h**, **7i**, **8h** and **8i** could be as effective as posaconazole and VT-1161, the most potent antifungal inhibitors of this target structure.

4 | EXPERIMENTAL SECTION

4.1 | General methods

The ^{1}H NMR and ^{13}C NMR spectra of the compounds were recorded on an Agilent Annual Refill (400 MHz) spectrometer (Santa Clara, California) at 400 and 100 MHz, respectively, in deuterated chloroform ($CDCl_3$) and dimethyl sulfoxide (DMSO), with tetramethylsilane (TMS) as an internal reference. Chemical shift values were recorded in parts per million (δ) and the designation of the signals were as follows: s, singlet; bs, broad singlet; d, doublet; t, triplet; q, quartet; and m, multiplet. The ESI (+) method and a Thermo TSQ Quantum Access device (Thermo Fisher Scientific Inc., Waltham, Massachusetts)

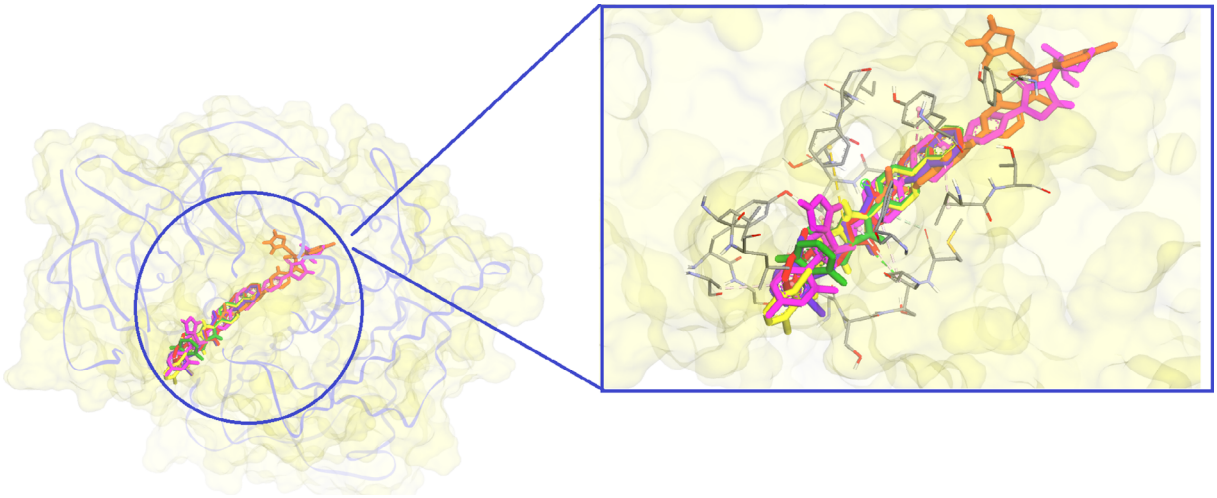

FIGURE 3 Superimposed 3D representations of the binding regions of the synthesized compounds, posaconazole and VT-1161 to the 5TZ1 target structure [Colour figure can be viewed at wileyonlinelibrary.com]

TABLE 6 Interacting residues and interaction types for compounds **7h**, **7i**, **8h**, **8i**, posaconazole, and VT-1161

Compounds	Binding affinity	Hydrogen bond	Electrostatic	Hydrophobic	Halogen	Other
7h	−11.5	1 Ser507^{CaHB}	2 His377^{PiCa}	1 Tyr118^{PS}, 2 His377^{PT}, 1 Phe233^{PT}, 1 Ala60^{APS}, 2 Pro230^{PA}, 2 Leu121^{PA}, 1 Ala61^{PA}		1 His377^{PiSu}, 1 Met508 ^{PiSu}
7i	−11.0	1 Met508^{CaHB}	1 His377^{PiCa}	2 Tyr118^{PS}, 1 His377^{PT}, 2 Pro230^{PA}, 1 Leu121^{PA}, 1 Ala61^{PA}, 1 Leu376^{PA}		1 His377^{PiSu}, 1 Phe380 ^{PiSu}
8h	−11.7		2 His377^{PiCa}	1 Tyr118^{PS}, 2 His377^{PT}, 1 Phe233^{PT}, 2 Pro230^{PA}, 1 Leu121^{PA}, 1 Leu87^{PA}, Leu88^{Pa}	1 Pro230	1 His377^{PiSu}, 1 Met508 ^{PiSu}
8i	−11.2	1 Gly65^{CaHB}, 1 Met508^{CaHB}	1 His377^{PiCa}	2 Tyr118^{PS}, 1 His377^{PT}, 2 Pro230^{PA}, 1 Leu121^{PA}, 1 Ala61^{PA}, 1 Leu376^{PA}, 1 Leu87^{PA}		1 His377^{PiSu}, 1 Phe380 ^{PiSu}
Posaconazole	−11.3			1 Tyr118^{PiS}, 1 Leu88^{PiS}, 1 Ile131^{PiS}, 1 Leu121^{A}, 1 Ile131^{A}, 1 Leu300^{A}, 1 Ile304^{A}, 1 Lys143^{A}, 1 Ile471^{A}, 1 Pro230^{A}, 1 Ala61^{PA}, 2 Leu87^{PA}	1 Pro230	1 Met508 ^{PiSu}
VT-1161	−11.8	1 Ty123^{CoHB}, 1 His468^{CoHB}	1 Lys143^{PiCa}	1 Ile304^{PiS}, 2 Tyr132^{PT}, 1 Leu139^{PA}, 1 Ile131^{PA}, 1 Lys143^{PA}, 1 Leu121^{PA}, 1 Phe233^{PA}, 1 Phe380^{PA}	1 Gln142, 1 Ser378	

Abbreviations: A, Alkyl; APS, Amide-Pi Stacked; CaHB, Carbon Hydrogen Bond; CoHB, Conventional Hydrogen Bond; PA, Pi-Alkyl; PiCa, Pi-Cation; PiS, Pi-Sigma; PiSu, Pi-Sulfur; PS, Pi-Pi Stacked; PT, Pi-Pi T-shaped.

were used to determine the mass spectrum. The FTIR spectra of the compounds were measured in attenuated total reflectance (ATR) on a Thermo Fisher Nicolet iS5 spectrometer (Thermo Fisher Scientific Inc.). Elemental analyses were performed using a LECO 932 CHNS (Leco Corp., St. Joseph, Michigan) instrument, and the results were within ±0.4% of the theoretical values. X-ray analyses were performed using a Bruker D8 QUEST device (Billerica, Massachusetts). The melting points of the compounds were determined using a Thermo Fisher IA9000 Digital Melting Point Apparatus (Thermo Fisher Scientific Inc.).

4.2 | Synthesis

4.2.1 | General procedure for the synthesis of 2-amino-1,3,4-thiadiazole derivatives (4 and 5)

Compounds **4** and **5** were synthesized according to a method given in the literature.[33–36]

4.2.2 | 5-((2,6-Dichlorobenzyl)thio)-1,3,4-thiadiazol-2-amine (4)

White solid, yield: 26.59 g (91%), m.p. 175 to 177°C (EtOH). FT-IR (ATR, cm^{-1}): 3263 to 3074 (—NH_2), 3052 (Ar-CH), 2944 (Aliph. CH), 1616 (C═N). ^{1}H NMR (400 MHz, DMSO-d_6), δ: 4.42 (s, 2H, —CH_2), Ar-H [7.33 (t, J = 8.0 Hz, 1H) 7.46 (d, J = 8.0 Hz, 2H)], 7.42 (s, 2H, NH_2). ^{13}C NMR (100 MHz, DMSO-d_6), δ: 35.99 (—CH_2), Ar-C [129.15 (CH), 130.73 (CH), 133.13 (C), 135.40 (C)], Thiadiazole-C [147.62 (C), 171.76 (C)]. Anal. (% calculated/found) for ($C_9H_7Cl_2N_3S_2$) (Mw: 292.21) C: 36.99/36.89; H: 2.41/2.37; N: 14.38/14.29. MS (ESI-m/z): 291.70 (M^+, 72).

4.2.3 | 5-((2,6-Difluorobenzyl)thio)-1,3,4-thiadiazol-2-amine (5)

White solid, yield: 24.11 g (93%), m.p. 162 to 164°C (EtOH). FT-IR (ATR, cm^{-1}): 3271 to 3081 (—NH_2), 3057 (Ar-CH), 2949 (Aliph. CH), 1626 (C═N). ^{1}H NMR

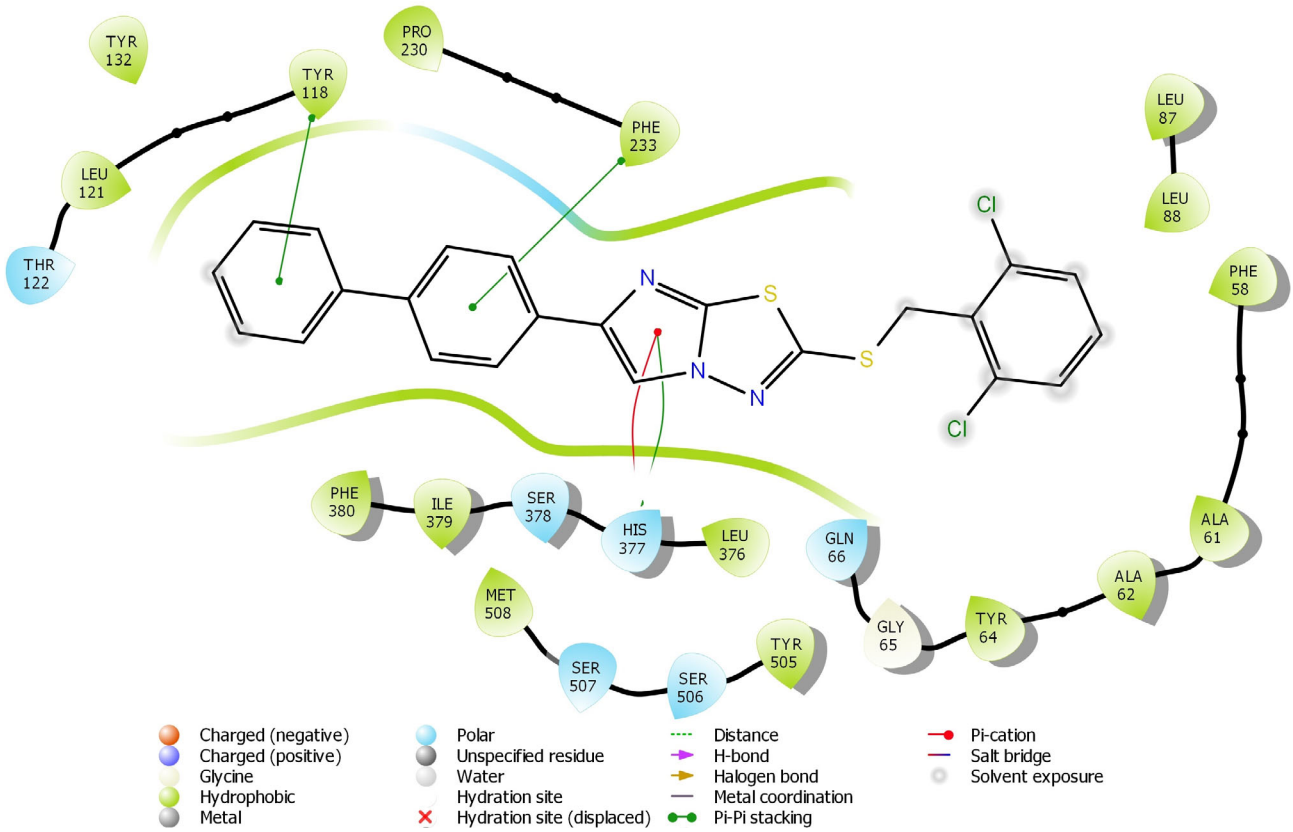

FIGURE 4 2D docking pose of compound **7h** inside the active site of 5TZ1 [Colour figure can be viewed at wileyonlinelibrary.com]

(400 MHz, DMSO-d_6), δ: 4.21 (s, 2H, —CH_2), Ar-H [7.08 (t, J = 8.0 Hz, 2H), 7.37 (d, J = 8.0 Hz, 1H)], 7.38 (s, 2H, NH_2). ^{13}C NMR (100 MHz, DMSO-d_6), δ: 27.36 (—CH_2), Ar-C [112.03-112.22 (CH) ^2J CF = 19.0 Hz, 113.69-113.88 (C) ^2J CF = 19.0 Hz, 130.69-130.79 (CH) ^3J CF = 9.9 Hz, 159.81-162.20 (C) ^1J CF = 239.0 Hz], Thiadiazole-C [147.81 (C), 171.60 (C)]. Anal. (% calculated/found) for ($C_9H_7F_2N_3S_2$) (Mw: 259.30) C: 41.69/41.58; H: 2.72/2.67; N: 16.21/16.17. MS (ESI-m/z): 259.92 (M^+, 64).

4.2.4 | General procedure for the synthesis of 2,6-disubstituted imidazo[2,1-*b*][1,3,4]thiadiazole derivatives (7a-7i and 8a-8i)

2-Amino-1,3,4-thiadiazole derivatives (**4** and **5**) (4 mmol) were dissolved with ethyl alcohol (50 mL) in a 100-mL 2-necked flask. Next, phenacyl bromide derivatives (**6a-6i**) (4 mmol) were dissolved with absolute ethyl alcohol and added to this solution dropwise using a dropping funnel. The mixture was heated and stirred for 12 hours. Thin-layer chromatography (TLC) was used to observe the progress of the reaction. When the reaction was completed, the solvent was evaporated using a rotary evaporator. The solution was then made slightly basic with a diluted Na_2CO_3 solution. The mixture was filtered and washed with plenty of water. The substance was purified by crystallized with acetone and then the pure substance was dried in a P_2O_5 vacuum oven. Finally, the structures of the compounds were characterized using various analysis techniques. The spectral data and the physical properties of the target compounds (**7a-7i** and **8a-8i**) are listed below.

4.2.5 | 2-((2,6-Dichlorobenzyl)thio)-6-phenylimidazo[2,1-*b*][1,3,4]thiadiazole (7a)

Light yellow crystals, yield: 1.11 g (71%), m.p. 126 to 128°C (Acetone); FT-IR (ATR, cm^{-1}): 3061 (Ar-CH), 2987 (Aliph. CH), 1599 (C═N). ^{1}H NMR (400 MHz, DMSO-d_6), δ: 4.70 (s, 2H, —CH_2), Ar-H [7.27 (t, J = 7.2 Hz, 1H), 7.39 (t, J = 7.2 Hz, 3H), 7.52 (d, J = 8.0 Hz, 2H), 7.85 (d, J = 8.0 Hz, 2H)], Imidazole-H [8.70 (s, 1H)]. ^{13}C NMR (100 MHz, DMSO-d_6), δ: 36.78 (—CH_2), Ar-C [125.14 (CH), 127.91 (CH), 129.14 (CH), 129.35 (CH), 131.33

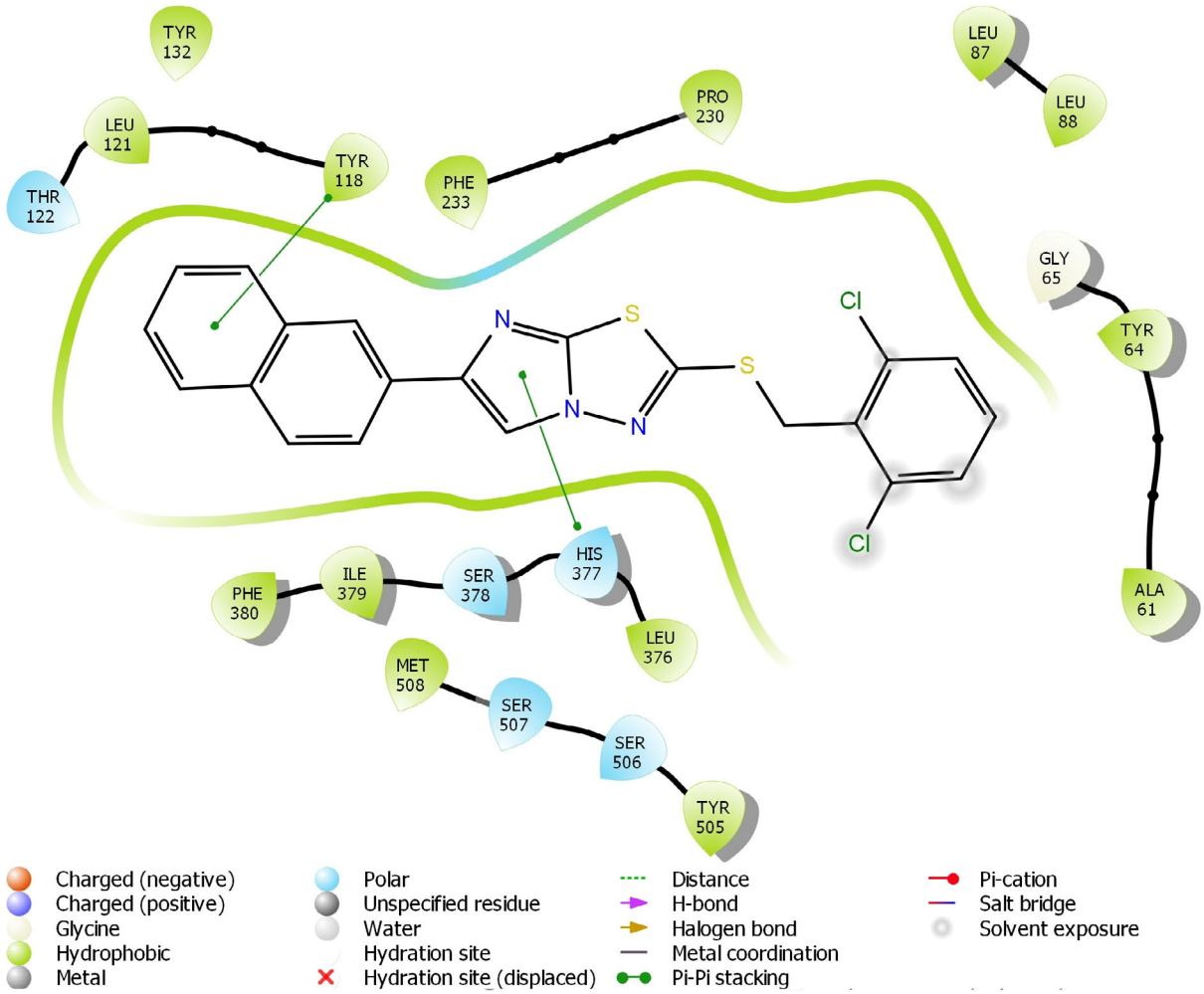

FIGURE 5 2D docking pose of compound **7i** inside the active site of 5TZ1 [Colour figure can be viewed at wileyonlinelibrary.com]

(CH), 132.09 (C), 134.03 (C), 135.57 (C)], Imidazole-C [111.17 (CH), 145.78 (C)], Thiadiazole-C [145.66 (C), 157.60 (C)]. Anal. (% calculated/found) for ($C_{17}H_{11}Cl_2N_3S_2$) (Mw: 392.33) C: 52.04/51.99; H: 2.83/2.77; N: 10.71/10.61. MS (ESI-*m/z*): 393.90 (M + 1, 70).

4.2.6 | 6-(4-Bromophenyl)-2-((2,6-dichlorobenzyl)thio)imidazo[2,1-*b*][1,3,4]thiadiazole (7b)

White solid, yield: 1.34 g (71%), m.p. 177 to 179°C (Acetone); FT-IR (ATR, cm^{-1}): 3088 (Ar-CH), 2960 (Aliph. CH), 1602 (C═N). ^{1}H NMR (400 MHz, DMSO-d_6), δ: 4.62 (s, 2H, —CH_2), Ar-H [7.39 (t, J = 7.2 Hz, 1H), 7.52 (d, J = 8.0 Hz, 2H), 7.85 (d, J = 8.0 Hz, 2H), 7.96 (d, J = 8.0 Hz, 2H)], Imidazole-H [8.72 (s, 1H)]. ^{13}C NMR (100 MHz, DMSO-d_6), δ: 36.24 (—CH_2), Ar-C [126.02 (CH), 129.18 (CH), 130.85 (CH), 131.49 (CH), 131.55 (C), 132.56 (C), 133.06 (CH), 135.59 (C)], Imidazole-C [111.57 (CH), 145.52 (C)], Thiadiazole-C [152.83 (C), 162.76 (C)]. Anal. (% calculated/found) for ($C_{17}H_{10}BrCl_2N_3S_2$) (Mw: 471.22) C: 43.33/43.26; H: 2.14/2.07; N: 8.92/8.82. MS (ESI-*m/z*): 489.64 (M + H_2O, 100).

4.2.7 | 6-(4-Chlorophenyl)-2-((2,6-dichlorobenzyl)thio)imidazo[2,1-*b*][1,3,4]thiadiazole (7c)

Yellowish solid, yield: 1.16 g (68%), m.p. 155 to 157°C (Acetone); FT-IR (ATR, cm^{-1}): 3058 (Ar-CH), 2994 (Aliph. CH), 1565 (C═N). ^{1}H NMR (400 MHz, DMSO-d_6), δ: 4.70 (s, 2H, —CH_2), Ar-H [7.39 (t, J = 7.2 Hz, 1H), 7.45 (d, J = 8.0 Hz, 2H), 7.52 (d, J = 8.0 Hz, 2H), 7.86 (d, J = 8.0 Hz, 2H)], Imidazole-H [8.75 (s, 1H)]. ^{13}C NMR (100 MHz, DMSO-d_6), δ: 35.74 (—CH_2), Ar-C [126.79 (CH), 129.19 (CH), 129.35 (CH), 131.35 (CH), 131.96 (C), 132.27 (C), 132.96 (C), 135.57 (C)], Imidazole-C [111.58

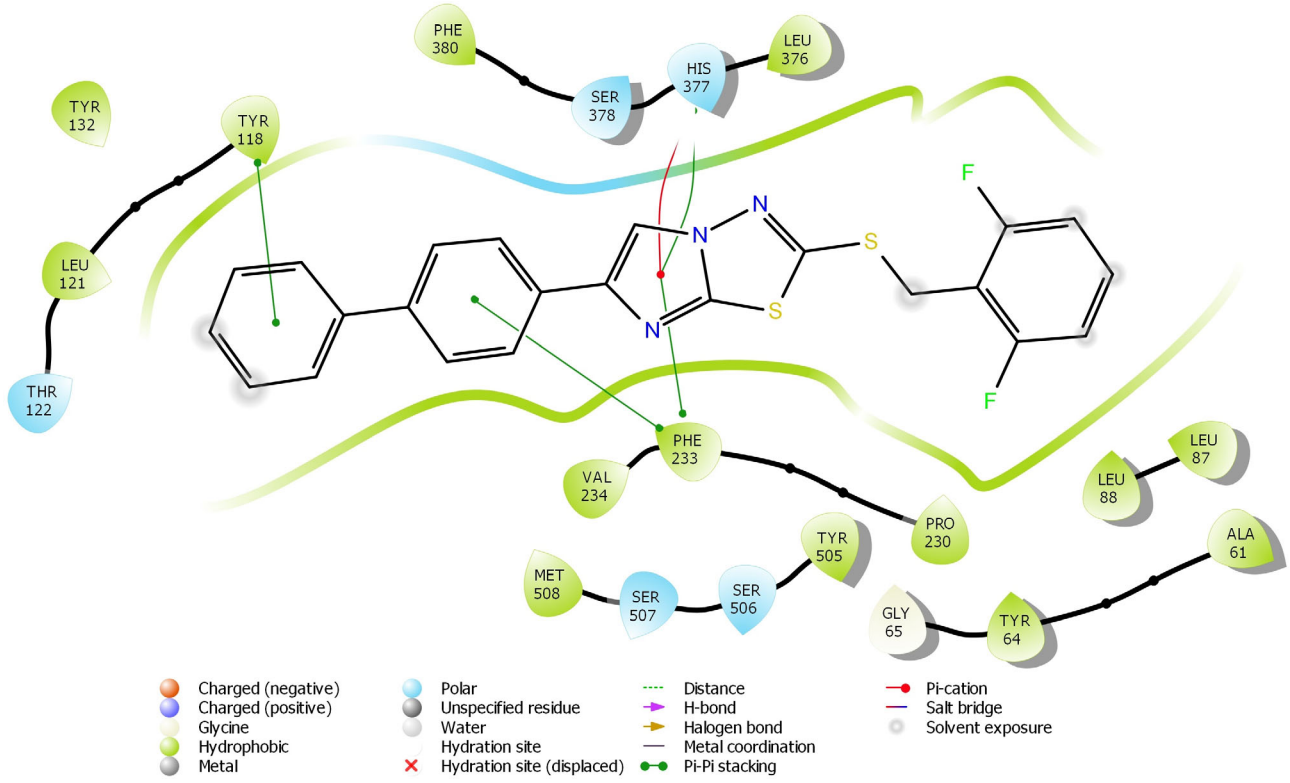

FIGURE 6 2D docking pose of compound **8h** inside the active site of 5TZ1 [Colour figure can be viewed at wileyonlinelibrary.com]

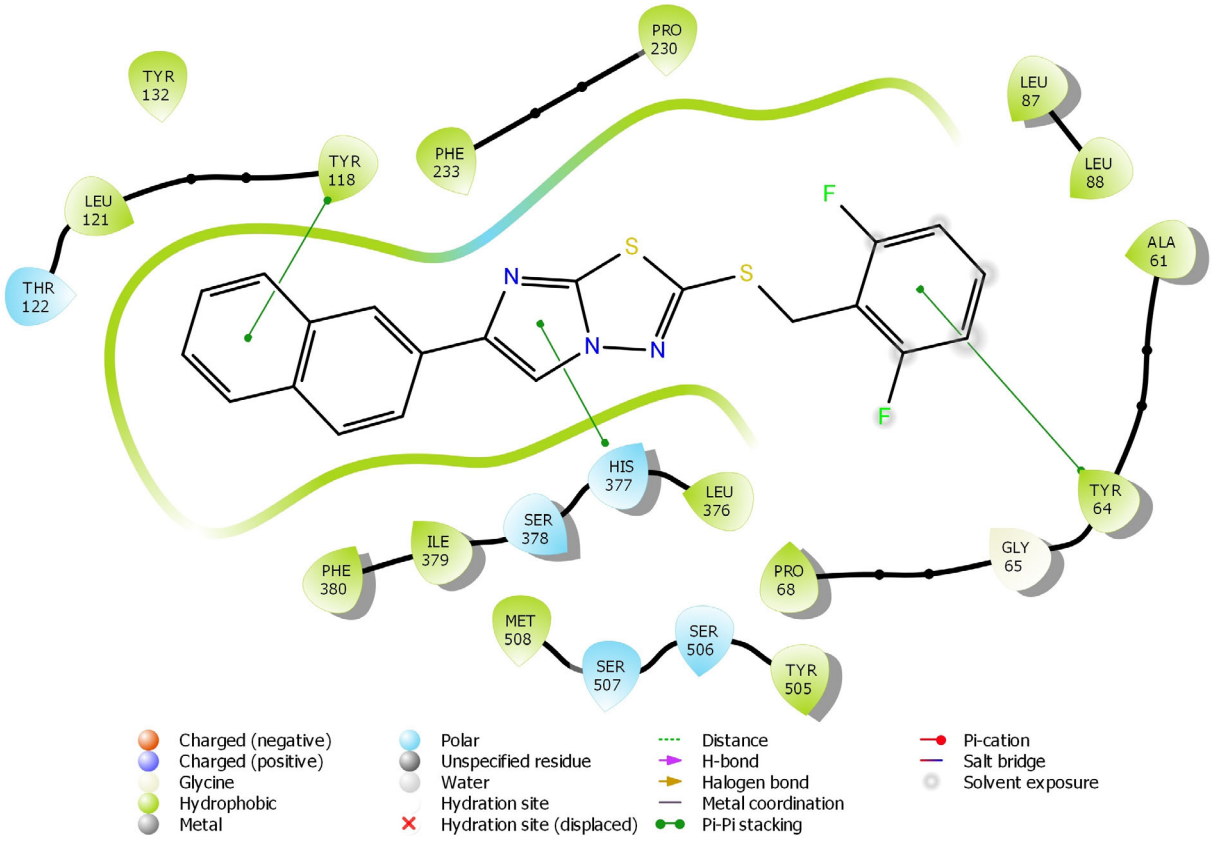

FIGURE 7 2D docking pose of compound **8i** inside the active site of 5TZ1 [Colour figure can be viewed at wileyonlinelibrary.com]

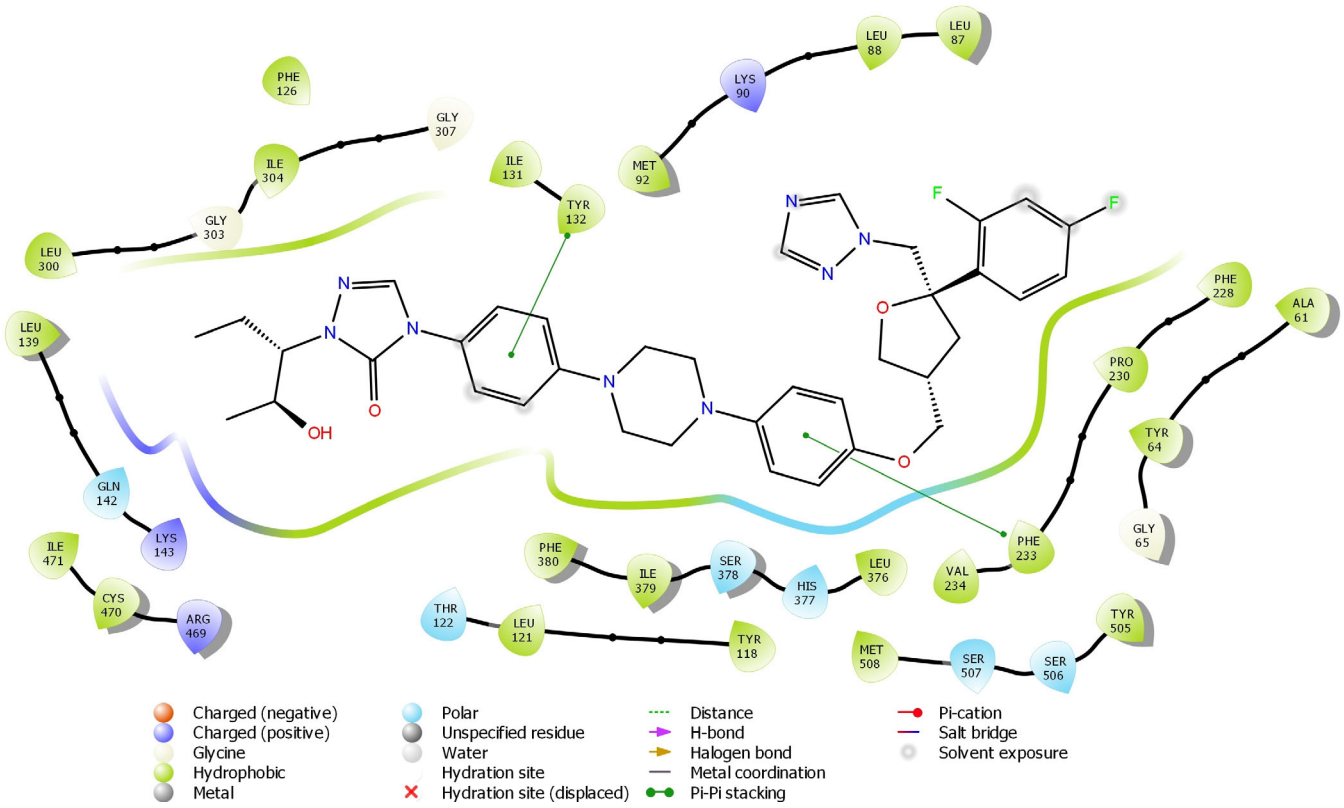

FIGURE 8 2D docking pose of posaconazole inside the active site of 5TZ1 [Colour figure can be viewed at wileyonlinelibrary.com]

(CH), 145.98 (C)], Thiadiazole-C [144.44 (C), 158.03 (C)]. Anal. (% calculated/found) for ($C_{17}H_{10}Cl_3N_3S_2$) (Mw: 426.77) C: 47.84/47.75; H: 2.36/2.29; N: 9.85/9.78. MS (ESI-*m/z*): 427.92 (M + 1, 65).

4.2.8 | 2-((2,6-Dichlorobenzyl)thio)-6-(4-fluorophenyl)imidazo[2,1-b][1,3,4] thiadiazole (7d)

Light crystals, yield: 1.23 g (75%), m.p. 149 to 151°C (Acetone); FT-IR (ATR, cm^{-1}): 3068 (Ar-CH), 2941 (Aliph. CH), 1594 (C═N). ^{1}H NMR (400 MHz, DMSO-d_6), δ: 4.70 (s, 2H, —CH_2), Ar-H [7.24 (t, J = 12.0 Hz, 2H), 7.40 (t, J = 8.0 Hz, 1H), 7.52 (d, J = 8.0 Hz, 2H), 7.88 (t, J = 12.0 Hz, 2H)], Imidazole-H [8.69 (s, 1H)]. ^{13}C NMR (100 MHz, DMSO-d_6), δ: 35.79 (—CH_2), Ar-C [115.94-116.15 (CH) ^2J CF = 21 Hz, 127.03–127.11 (CH) ^3J CF = 8.3 Hz, 129.35 (CH), 130.57-130.60 (C) ^4J CF = 3.0 Hz, 131.33 (CH), 132.01 (C), 135.56 (C), 158.65-160.83 (C) ^1J CF = 218.0 Hz], Imidazole-C [111.02 (CH), 145.83 (C)], Thiadiazole-C [144.75 (C), 163.26 (C)]. Anal. (% calculated/found) for ($C_{17}H_{10}Cl_2FN_3S_2$) (Mw: 410.32) C: 49.76/49.68; H: 2.46/2.37; N: 10.24/10.18. MS (ESI-*m/z*): 409.72 (M^+, 90).

4.2.9 | 2-((2,6-Dichlorobenzyl)thio)-6-(4-methoxyphenyl)imidazo[2,1-*b*][1,3,4] thiadiazole (7e)

White solid, yield: 1.21 g (72%), m.p. 152 to 153°C (Acetone); FT-IR (ATR, cm^{-1}): 3061 (Ar-CH), 2987 (Aliph. CH), 1611 (C═N). ^{1}H NMR (400 MHz, DMSO-d_6), δ: 3.76 (s, 3H, —OCH_3), 4.68 (s, 2H, —CH_2), Ar-H [6.96 (d, J = 8.0 Hz, 2H), 7.39 (t, J = 8.0 Hz, 1H), 7.52 (d, J = 8.0 Hz, 2H), 7.77 (d, J = 8.0 Hz, 2H)], Imidazole-H [8.58 (s, 1H)]. ^{13}C NMR (100 MHz, DMSO-d_6), δ: 35.90 (—CH_2), 55.58 (—OCH_3), Ar-C [114.58 (CH), 126.49 (C), 126.66 (CH), 129.34 (CH), 131.30 (CH), 132.10 (C), 135.54 (C), 156.84 (C)], Imidazole-C [110.02 (CH), 145.77 (C)], Thiadiazole-C [145.57 (C), 159.26 (C)]. Anal. (% calculated/found) for ($C_{18}H_{13}Cl_2N_3OS_2$) (Mw: 422.35) C: 51.19/51.08; H: 3.10/3.05; N: 9.95/9.84. MS (ESI-*m/z*): 421.74 (M^+, 100).

4.2.10 | 2-((2,6-Dichlorobenzyl)thio)-6-(4-nitrophenyl)imidazo[2,1-*b*][1,3,4] thiadiazole (7f)

Yellow solid, yield: 1.17 g (67%), m.p. 222 to 224°C (Acetone); FT-IR (ATR, cm^{-1}): 3069 (Ar-CH), 2918

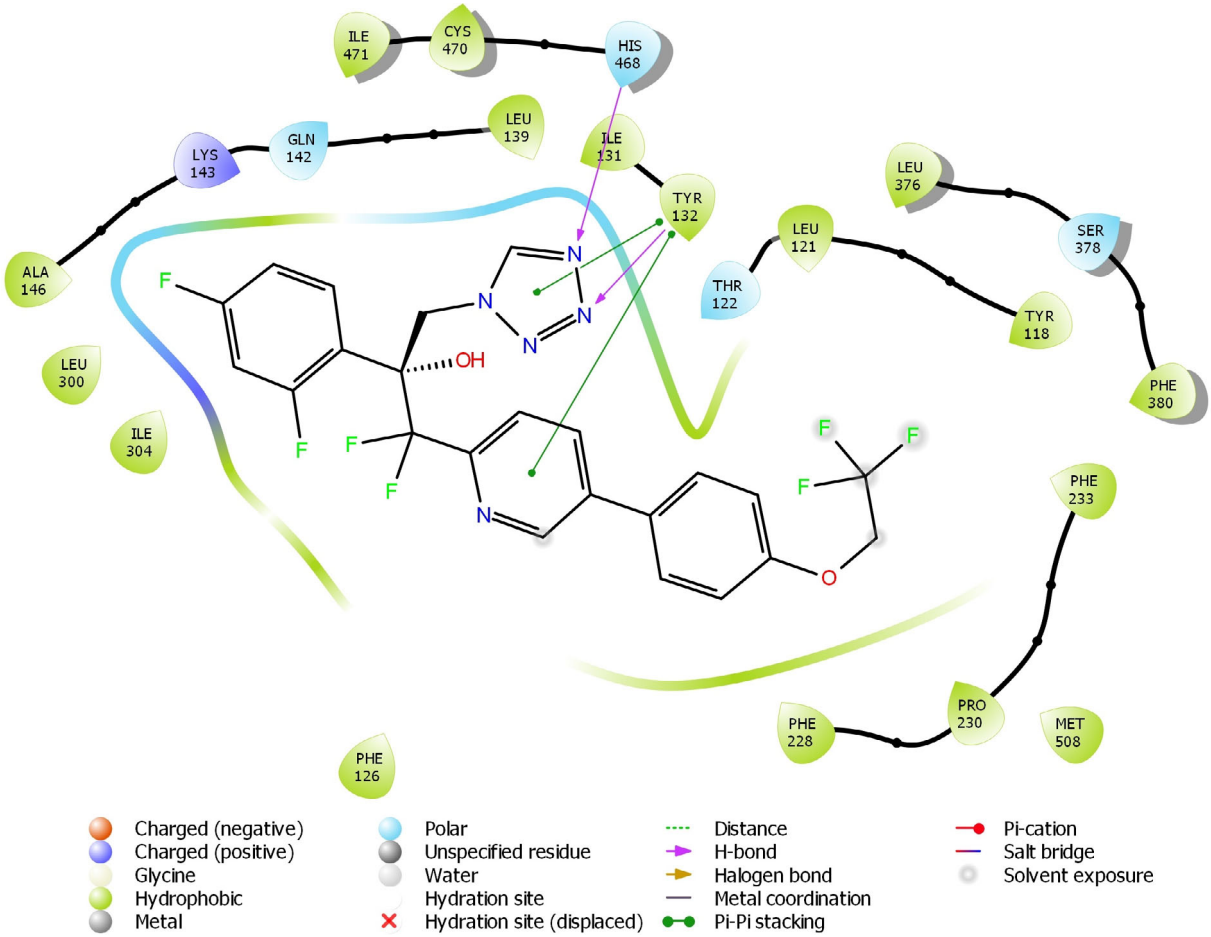

FIGURE 9 2D docking pose of VT-1161 inside the active site of 5TZ1 [Colour figure can be viewed at wileyonlinelibrary.com]

(Aliph. CH), 1638 (C═N). ^{1}H NMR (400 MHz, DMSO-d_6), δ: 4.74 (s, 2H, —CH_2), Ar-H [7.40 (t, J = 8.0 Hz, 1H), 7.53 (d, J = 8.0 Hz, 2H), 8.10 (dd, J = 12.0 Hz, 8.0 Hz, 2H), 8.26 (dd, J = 12.0 Hz, 8.0 Hz, 2H)], Imidazole-H [8.99 (s, 1H)]. ^{13}C NMR (100 MHz, DMSO-d_6), δ: 35.56 (—CH_2), Ar-C [124.46 (CH), 125.78 (CH), 129.38 (CH), 130.38 (CH), 131.49 (C), 135.59 (C), 140.68 (C), 152.86 (C)], Imidazole-C [113.81 (CH), 143.35 (C)], Thiadiazole-C [151.05 (C), 159.45 (C)]. Anal. (% calculated/found) for ($C_{17}H_{10}Cl_2N_4O_2S_2$) (Mw: 437.32) C: 46.69/46.60; H: 2.30/2.22; N: 12.81/12.74. MS (ESI-m/z): 454.79 (M + H_2O, 100).

4.2.11 | 4-(2-((2,6-Dichlorobenzyl)thio) imidazo[2,1-*b*][1,3,4]thiadiazol-6-yl) benzonitrile (7g)

White solid, yield: 1.16 g (70%), m.p. 203 to 204°C (Acetone); FT-IR (ATR, cm^{-1}): 3101 (Ar-CH), 2957 (Aliph. CH), 2225 (C≡N), 1622 (C═N). ^{1}H NMR (400 MHz, DMSO-d_6), δ: 4.63 (s, 2H, —CH_2), Ar-H [7.40 (t, J = 12.0 Hz, 1H), 7.52 (d, J = 8.0 Hz, 2H), 8.11 (dd, J = 8.0 Hz, 8.0 Hz, 2H), 8.18 (dd, J = 8.0 Hz, 8.0 Hz, 2H)], Imidazole-H [8.93 (s, 1H)]. ^{13}C NMR (100 MHz, DMSO-d_6), δ: 35.60 (—CH_2), 119.44 (C≡N), Ar-C [113.20 (C), 125.61 (CH), 129.37 (CH), 131.55 (CH), 133.23 (C), 133.40 (CH), 135.59 (C), 138.57 (C)], Imidazole-C [109.92 (CH), 146.50 (C)], Thiadiazole-C [143.73 (C), 159.10 (C)]. Anal. (% calculated/found) for ($C_{18}H_{10}Cl_2N_4S_2$) (Mw: 417.33) C: 51.80/51.74; H: 2.42/2.36; N: 13.42/13.30. MS (ESI-m/z): 440.99 (M + Na, 100).

4.2.12 | 6-([1,1′-Biphenyl]-4-yl)-2-((2,6-dichlorobenzyl)thio)imidazo[2,1-*b*] [1,3,4]thiadiazole (7h)

Yellowish solid, yield: 1.29 g (69%), m.p. 198 to 200°C (Acetone); FT-IR (ATR, cm^{-1}): 3076 (Ar-CH), 2981 (Aliph. CH), 1560 (C═N). ^{1}H NMR (400 MHz, DMSO-d_6), δ: 4.72 (s, 2H, —CH_2), Ar-H [7.36 (t, J = 8.0 Hz, 1H), 7.41 (t, J = 8.0 Hz, 1H), 7.46 (t, J = 7.2 Hz, 2H), 7.53 (d, J = 8.0 Hz, 2H), 7.71 (t, J = 6.0 Hz, 4H), 7.94 (d,

J = 8.0 Hz, 2H)], imidazole-H [8.77 (s, 1H)]. ^{13}C NMR (100 MHz, DMSO-d_6), δ: 36.63 (—CH_2), Ar-C [125.69 (CH), 126.92 (CH), 127.40 (CH), 127.79 (CH), 129.41 (CH), 129.63 (CH), 131.36 (CH), 132.02 (C), 133.37 (C), 135.57 (C), 139.49 (C), 140.16 (C)], imidazole-C [111.35 (CH), 145.65 (C)], Thiadiazole-C [145.23 (C), 158.46 (C)]. Anal. (% calculated/found) for ($C_{23}H_{15}Cl_2N_3S_2$) (Mw: 468.42) C: 58.97/58.89; H: 3.23/3.16; N: 8.97/8.88. MS (ESI-m/z): 469.90 (M + 1, 85).

4.2.13 | 2-((2,6-Dichlorobenzyl)thio)-6-(naphthalen-2-yl)imidazo[2,1-*b*][1,3,4]thiadiazole (7i)

Yellowish solid, yield: 1.17 g (66%), m.p. 160 to 162°C (Acetone); FT-IR (ATR, cm^{-1}): 3052 (Ar-CH), 2987 (Aliph. CH), 1565 (C═N). ^{1}H NMR (400 MHz, DMSO-d_6), δ: 4.72 (s, 2H, —CH_2), Ar-H [7.40 (t, J = 8.0 Hz, 1H), 7.47-7.50 (m, 2H), 7.53 (d, J = 8.0 Hz, 2H), 7.83–7.94 (m, 3H), 7.99 (d, J = 8.0 Hz, 1H)], 8.39 (s, 1H), imidazole-H [8.83 (s, 1H)]. ^{13}C NMR (100 MHz, DMSO-d_6), δ: 35.80 (—CH_2), Ar-C [123.34 (CH), 123.82 (CH), 126.34 (CH), 126.95 (CH), 128.10 (CH), 128.40 (CH), 128.69 (CH), 129.35 (CH), 131.34 (CH), 131.52 (C), 132.02 (C), 132.90 (C), 133.66 (C), 135.58 (C)], imidazole-C [111.71 (CH), 146.07 (C)], thiadiazole-C [145.65 (C), 157.71 (C)]. Anal. (% calculated/found) for ($C_{21}H_{13}Cl_2N_3S_2$) (Mw: 442.38) C: 57.01/56.94; H: 2.96/2.89; N: 9.50/9.42. MS (ESI-m/z): 441.97 (M^+, 100).

4.2.14 | 2-((2,6-Difluorobenzyl)thio)-6-phenylimidazo[2,1-*b*][1,3,4]thiadiazole (8a)

Yellowish solid, yield: 1.06 g (74%), m.p. 217 to 218°C (Acetone); FT-IR (ATR, cm^{-1}): 3049 (Ar-CH), 2992 (Aliph. CH), 1592 (C═N). ^{1}H NMR (400 MHz, DMSO-d_6), δ: 4.52 (s, 2H, —CH_2), Ar-H [7.12 (t, J = 8.0 Hz, 2H), 7.27 (t, J = 8.0 Hz, 1H), 7.38 (d, J = 8.0 Hz, 1H), 7.43 (q, J = 8.0 Hz, 2H), 7.84 (d, J = 8.0 Hz, 2H)], imidazole-H [8.69 (s, 1H)]. ^{13}C NMR (100 MHz, DMSO-d_6), δ: 27.06 (—CH_2), Ar-C [112.17-112.36 (CH) ^2J CF = 19.0 Hz, 112.62-112.85 (CH) ^2J CF = 21.5 Hz, 125.14 (CH), 126.66 (CH), 127.93 (CH), 129.08-129.14 (CH) ^3J CF = 6.1 Hz, 131.21 (CH), 133.96 (C), 159.77-162.25 (C) ^1J CF = 240 Hz], Imidazole-C [111.15 (CH), 145.60 (C)], Thiadiazole-C [144.91 (C), 162.32 (C)]. Anal. (% calculated/found) for ($C_{17}H_{11}F_2N_3S_2$) (Mw: 359.42) C: 56.81/56.72; H: 3.08/3.00; N: 11.69/11.60. MS (ESI-m/z): 359.60 (M^+, 65).

4.2.15 | 6-(4-Bromophenyl)-2-((2,6-difluorobenzyl)thio)imidazo[2,1-*b*][1,3,4]thiadiazole (8b)

White solid, yield: 1.29 g (74%), m.p. 204 to 206°C (Acetone); FT-IR (ATR, cm^{-1}): 3082 (Ar-CH), 2914 (Aliph. CH), 1580 (C═N). ^{1}H NMR (400 MHz, DMSO-d_6), δ: 4.53 (s, 2H, —CH_2), Ar-H [7.12 (t, J = 8.0 Hz, 2H), 7.43 (t, J = 8.0 Hz, 1H), 7.58 (d, J = 8.0 Hz, 2H), 7.79 (d, J = 8.0 Hz, 2H)], Imidazole-H [8.74 (s, 1H)]. ^{13}C NMR (100 MHz, DMSO-d_6), δ: 27.00 (—CH_2), Ar-C [112.17-112.37 (CH) ^2J CF = 19.0 Hz, 112.42-112.62 (CH) ^2J CF = 19.8 Hz, 120.80 (C), 127.10 (CH), 128.48 (CH), 131.33-131.43 (CH) ^3J CF = 9.9 Hz, 132.08 (C), 133.31 (CH), 159.85-162.25 (C) ^1J CF = 240.0 Hz], imidazole-C [111.58 (CH), 145.81 (C)], thiadiazole-C [144.40 (C), 162.32 (C)]. Anal. (% calculated/found) for ($C_{17}H_{10}BrF_2N_3S_2$) (Mw: 438.31) C: 46.58/46.46; H: 2.30/2.22; N: 9.59/9.50. MS (ESI-m/z): 439.89 (M + 1, 100).

4.2.16 | 6-(4-Chlorophenyl)-2-((2,6-difluorobenzyl)thio)imidazo[2,1-*b*][1,3,4]thiadiazole (8c)

White solid, yield: 1.15 g (73%), m.p. 148 to 149°C (Acetone); FT-IR (ATR, cm^{-1}): 3027 (Ar-CH), 2983 (Aliph. CH), 1592 (C═N). ^{1}H NMR (400 MHz, DMSO-d_6), δ: 4.53 (s, 2H, —CH_2), Ar-H [7.12 (t, J = 8.0 Hz, 2H), 7.45 (d, J = 8.0 Hz, 3H), 7.85 (d, J = 8.0 Hz, 2H)], imidazole-H [8.72 (s, 1H)]. ^{13}C NMR (100 MHz, DMSO-d_6), δ: 27.00 (—CH_2), Ar-C [112.18-112.36 (CH) ^2J CF = 18.3 Hz, 112.42-112.62 (CH) ^2J CF = 20.5 Hz, 126.78 (CH), 129.17 (CH), 131.22 (CH), 131.33-131.43 (CH) ^3J CF = 10.6 Hz, 132.24 (C), 132.96 (C), 159.85-162.25 (C) ^1J CF = 240.0 Hz], imidazole-C [111.54 (CH), 145.80 (C)], thiadiazole-C [144.40 (C), 159.85-162.33 (C)]. Anal. (% calculated/found) for ($C_{17}H_{10}ClF_2N_3S_2$) (Mw: 393.86) C: 51.84/51.76; H: 2.56/2.48; N: 10.67/10.60. MS (ESI-m/z): 393.83 (M^+, 100).

4.2.17 | 2-((2,6-Difluorobenzyl)thio)-6-(4-fluorophenyl)imidazo[2,1-*b*][1,3,4]thiadiazole (8d)

Light yellow crystals, yield: 1.19 g (79%), m.p. 147 to 148°C (Acetone); FT-IR (ATR, cm^{-1}): 3050 (Ar-CH), 2955 (Aliph. CH), 1587 (C═N). ^{1}H NMR (400 MHz, DMSO-d_6), δ: 4.52 (s, 2H, —CH_2), Ar-H [7.12 (t, J = 8.0 Hz, 2H),

7.22 (t, J = 8.0 Hz, 2H), 7.39-7.46 (m, 1H), 7.87 (t, J = 8.0 Hz, 2H)], imidazole-H [8.66 (s, 1H)]. ^{13}C NMR (100 MHz, DMSO-d_6), δ: 27.04 (—CH_2), Ar-C [112.15-112.34 (CH) ^2J CF = 18.9 Hz, 112.65-112.84 (CH) ^2J CF = 19.7 Hz, 115.91-116.13 (CH) ^2J CF = 22.0 Hz, 127.02-127.11 (C) ^3J CF = 8.4 Hz, 130.61 (CH), 131.30-131.40 (CH) ^3J CF = 9.9 Hz, 159.85-162.25 (C) ^1J CF = 240.0 Hz], imidazole-C [110.97 (CH), 145.64 (C)], thiadiazole-C [144.71 (C), 163.26 (C)]. Anal. (% calculated/found) for ($C_{17}H_{10}F_3N_3S_2$) (Mw: 377.41) C: 54.10/54.02; H: 2.67/2.59; N: 11.13/11.04. MS (ESI-m/z): 377.89 (M^+, 100).

4.2.18 | 2-((2,6-Difluorobenzyl)thio)-6-(4-methoxyphenyl)imidazo[2,1-b][1,3,4]thiadiazole (8e)

Light crystals, yield: 1.17 g (75%), m.p. 142 to 143°C (Acetone); FT-IR (ATR, cm^{-1}): 3048 (Ar-CH), 2976 (Aliph. CH), 1599 (C═N). ^{1}H NMR (400 MHz, DMSO-d_6), δ: 3.76 (s, 3H, —OCH_3), 4.51 (s, 2H, —CH_2), Ar-H [6.96 (d, J = 8.0 Hz, 2H), 7.12 (t, J = 8.0 Hz, 2H), 7.42 (t, J = 8.0 Hz, 1H), 7.76 (d, J = 8.0 Hz, 2H)], imidazole-H [8.56 (s, 1H)]. ^{13}C NMR (100 MHz, DMSO-d_6), δ: 27.16 (—CH_2), 55.58 (—OCH_3), Ar-C [112.15-112.34 (CH) ^2J CF = 18.9 Hz, 112.70-112.89 (CH) ^2J CF = 19 Hz, 114.57 (CH), 126.52 (C), 131.29-131.39 (CH) ^3J CF = 9.8 Hz, 159.77-162.24 (C) ^1J CF = 247.3 Hz], imidazole-C [110.01 (CH), 145.54 (C)], thiadiazole-C [145.36 (C), 162.32 (C)]. Anal. (% calculated/found) for ($C_{18}H_{13}F_2N_3OS_2$) (Mw: 389.44) C: 55.51/55.43; H: 3.36/3.29; N: 10.79/10.70. MS (ESI-m/z): 389.76 (M^+, 100).

4.2.19 | 2-((2,6-Difluorobenzyl)thio)-6-(4-nitrophenyl)imidazo[2,1-b][1,3,4]thiadiazole (8f)

Yellow solid, yield: 1.16 g (72%), m.p. 200 to 201°C (Acetone); FT-IR (ATR, cm^{-1}): 3098 (Ar-CH), 2919 (Aliph. CH), 1585 (C═N). ^{1}H NMR (400 MHz, DMSO-d_6), δ: 4.57 (s, 2H, —CH_2), Ar-H [7.15 (t, J = 8.0 Hz, 2H), 7.44 (t, J = 8.0 Hz, 1H), 8.10 (d, J = 8.0 Hz, 2H), 8.26 (d, J = 8.0 Hz, 2H)], Imidazole-H [8.97 (s, 1H)]. ^{13}C NMR (100 MHz, DMSO-d_6), δ: 27.04 (—CH_2), Ar-C [115.87-116.08 (CH) ^2J CF = 21.2 Hz, 124.67 (CH), 125.64 (CH), 131.68-131.77 (CH) ^3J CF = 8.4 Hz, 132.71 (CH), 143.04 (C), 158.85-161.39 (C) ^1J CF = 254.0 Hz], imidazole-C [113.70 (CH), 146.10 (C)], thiadiazole-C [146.54 (C), 163.35 (C)]. Anal. (% calculated/found) for ($C_{17}H_{10}F_2N_4O_2S_2$) (Mw: 404.41) C: 50.49/50.38; H: 2.49/2.40; N: 13.85/13.76. MS (ESI-m/z): 404.67 (M^+, 100).

4.2.20 | 4-(2-((2,6-Difluorobenzyl)thio)imidazo[2,1-b][1,3,4]thiadiazol-6-yl)benzonitrile (8g)

Light crystals, yield: 1.12 g (73%), m.p. 189 to 190°C (Acetone); FT-IR (ATR, cm^{-1}): 3033 (Ar-CH), 2928 (Aliph. CH), 2214 (C≡N), 1599 (C═N). ^{1}H NMR (400 MHz, DMSO-d_6), δ: 4.54 (s, 2H, —CH_2), Ar-H [7.12 (t, J = 12.0 Hz, 2H), 7.39-7.46 (m, 1H), 7.83 (d, J = 8.0 Hz, 2H), 8.00 (d, J = 8.0 Hz, 2H)], imidazole-H [8.87 (s, 1H)]. ^{13}C NMR (100 MHz, DMSO-d_6), δ: 26.81 (—CH_2), 119.45 (C≡N), Ar-C [109.88 (CH), 112.19-112.38 (CH) ^2J CF = 19.0 Hz, 112.24-112.52 (CH) ^2J CF = 28.0 Hz, 125.58 (CH), 131.36-131.46 (CH) ^3J CF = 10.6 Hz, 133.21 (CH), 138.57 (C), 159.80-162.26 (C) ^1J CF = 247.4 Hz], imidazole-C [113.20 (CH), 146.32 (C)], thiadiazole-C [143.67 (C), 162.34 (C)]. Anal. (% calculated/found) for ($C_{18}H_{10}F_2N_4S_2$) (Mw: 384.43) C: 56.24/56.12; H: 2.62/2.56; N: 14.57/14.50. MS (ESI-m/z): 384.65 (M^+, 100).

4.2.21 | 6-([1,1′-Biphenyl]-4-yl)-2-((2,6-difluorobenzyl)thio)imidazo[2,1-b][1,3,4]thiadiazole (8h)

White solid, yield: 1.27 g (73%), m.p. 182 to 184°C (Acetone); FT-IR (ATR, cm^{-1}): 3034 (Ar-CH), 2969 (Aliph. CH), 1593 (C═N). ^{1}H NMR (400 MHz, DMSO-d_6), δ: 4.54 (s, 2H, -CH_2), Ar-H [7.13 (t, J = 8.0 Hz, 2H), 7.35 (d, J = 8.0 Hz, 1H), 7.43 to 7.66 (m, 3H), 7.70 (bs, 4H), 7.93 (d, J = 8.0 Hz, 2H)], imidazole-H [8.74 (s, 1H)]. ^{13}C NMR (100 MHz, DMSO-d_6), δ: 27.06 (—CH_2), Ar-C [112.19-112.37 (CH) ^2J CF = 18.2 Hz, 112.43-112.67 (CH) ^2J CF = 24.3 Hz, 125.68 (CH), 126.91 (CH), 127.37 (CH), 127.90 (CH), 129.40 (CH), 131.22-131.33 (CH) ^3J CF = 10.6 Hz, 133.18 (CH), 139.47 (C), 140.11 (C), 159.86-162.26 (C) ^1J CF = 241 Hz], imidazole-C [111.31 (CH), 145.73 (C)], thiadiazole-C [145.26 (C), 162.34 (C)]. Anal. (% calculated/found) for ($C_{23}H_{15}F_2N_3S_2$) (Mw: 435.51) C: 63.43/63.48; H: 3.47/3.38; N: 9.65/9.59. MS (ESI-m/z): 435.61 (M^+, 100).

4.2.22 | 2-((2,6-Difluorobenzyl)thio)-6-(naphthalen-2-yl)imidazo[2,1-b][1,3,4]thiadiazole (8i)

Yellowish solid, yield: 1.20 g (73%), m.p. 130 to 131°C (Acetone); FT-IR (ATR, cm^{-1}): 3049 (Ar-CH), 2993 (Aliph. CH), 1585 (C═N). ^{1}H NMR (400 MHz, DMSO-d_6), δ: 4.54 (s, 2H, —CH_2), Ar-H [7.13 (t, J = 8.0 Hz, 2H), 7.43 (d, J = 8.0 Hz, 1H), 7.47-7.52 (m, 2H), 7.87-7.94 (m,

3H), 7.99 (d, J = 8.0 Hz, 1H), 8.38 (s, 1H)], imidazole-H [8.81 (s, 1H)]. ^{13}C NMR (100 MHz, DMSO-d_6), δ: 27.08 (—CH_2), Ar-C [112.19-112.37 (CH) ^2J CF = 18.2 Hz, 112.43-112.68 (CH) ^2J CF = 25.0 Hz, 123.32 (CH), 123.82 (CH), 126.33 (CH), 126.94 (CH), 128.10 (CH), 128.40 (CH), 128.68 (CH), 131.23-131.33 (CH) ^3J CF = 9.9 Hz, 131.51 (C), 132.90 (C), 133.65 (C), 159.87-162.27 (C) ^1J CF = 241 Hz], imidazole-C [111.67 (CH), 145.90 (C)], thiadiazole-C [145.60 (C), 162.35 (C)]. Anal. (% calculated/found) for ($C_{21}H_{13}F_2N_3S_2$) (Mw: 409.47) C: 61.60/61.50; H: 3.20/3.11; N: 10.26/10.18. MS (ESI-*m/z*): 409.78 (M^+, 100).

4.3 | Crystallographic analysis

The structure solution of the crystals was performed using direct methods in ShelXT.[51] In order to determine the positions of atoms other than hydrogen in the solution phase, the refinement process was performed with the ShelXL[52] program, which depends on the full-matrix least-squares method. Isotropic refinement was used in order to increase the sensitivity of the atom positions and determine the missing atoms in the first phase of the refinement. It was seen as a result of the refinement process that there were no missing atoms other than hydrogen. Next, anisotropic refinement was performed. In the following phase of the refinement, hydrogen atoms were determined. The positions of the hydrogen atoms were obtained geometrically from the difference-Fourier map of the electron density in the unit cell. When placing the hydrogen atoms geometrically, aromatic bond lengths were fixed at 0.93 Å, methylene C—H_2 bond lengths at 0.97 Å, and methyl C—H_3 bond lengths at 0.96 Å. After the structure solution and refinement process, the olex2[53] and MERCURY[54] programs were used for the molecular drawings and calculations. None of the crystals had the classical hydrogen bonding and the packaging of the crystals occurred through weak Van der Waals and pi-pi interactions.

5 | DETERMINATION OF THE IN VITRO ANTIFUNGAL ACTIVITIES

5.1 | Fungus cultures

Alternaria solani (isolated from tomatoes in Antalya, Turkey), *Fusarium oxysporum f.sp. melonis* (isolated from melon in Hatay, Turkey), and *Verticillium dahliae* (isolated from tomatoes in Antalya, Turkey) plant pathogens were used for this study. The pathogens were grown on potato dextrose agar (PDA) medium at 22 ± 2°C for about 7 days.

5.2 | In vitro antifungal activity test

Antifungal activity studies were determined using the agar plate method.[55] The compounds were dissolved in DMSO. The compounds were added to the PDA at 40°C to give final concentrations of 0.5, 1, 2, 4, 8, and 20 μg/mL for the compound, and then the PDA with the compounds were each poured (~10 mL/plate) into a Petri plate (60 mm in diameter). Seven-day-old agar discs (5 mm in diameter) bearing the desired fungus growth were transferred into the Petri plates. These fungus cultures were incubated at 22 ± 2°C for 7 days. Fungus growth was recorded daily. Commercial fungicide (Thiram 80%) was used as the positive control and DMSO was used as the negative control. The experiment was set up with three replications and repeated twice.

The percentage of mycelial growth inhibition was calculated according to the formula given below[56]:

$$\mathrm{MGI} = 100 \times (\mathrm{dc} - \mathrm{dt})/\mathrm{dc}$$

Here, MGI is the mycelial growth inhibition, dc is the mycelial growth in control, and dt is the mycelial growth in the compounds.

5.3 | Determination of the lethal dose, minimum fungicidal concentration, and minimum inhibitory concentration values

The minimum fungicidal concentration (MFC) and minimum inhibitory concentration (MIC) values were determined using the two-fold serial dilution method. The test compounds were dissolved in DMSO to obtain 40 μg/mL stock solutions. For the MIC and MFC assays, each compound was prepared at concentrations of 40, 20, 10, 5, 2.5, 1.25, and 0.625 μg/mL. In the laminar flow cabin, Whatman no. 1 sterile filter paper discs (6 mm) were impregnated with 50 μL of the compounds (corresponding to 40, 20, 10, 5, 2.5, 1.25, and 0.625 μg/mL of the compounds) and allowed to dry at room temperature (for 4 hours).[57] Next, the compound impregnated paper discs were placed on PDA medium in 90-mm sterile petri plates. Discs (5 mm in diameter) of 7-day-old culture of test fungi were inoculated into the centers of the Petri plates. All of the fungi were incubated at 22 ± 2°C. There was a distance of 25 mm between the mycelium discs and the paper discs. The obtained inhibition zones were recorded. The experiment was set up in three replicates and repeated two times. As a negative control, only DMSO was impregnated into discs. In the positive control, 80% thiram

(3000 μg/mL) was used against the test fungi at the recommended doses. The MIC was defined as the lowest test concentration that allowed no detectable mycelium growth. The MFC was defined as the lowest test concentration that allowed no mycelium growth of the organism on agar.[58] In addition, the median lethal dose (LD_{50}) values were calculated. Six different doses used in the calculation of the MIC were calculated using the results of the inhibition zones. Lethal dose estimates for the LD_{50} were determined using Polo Plus software (LeOra Software LLC., Northamptonshire, UK).

5.4 | Details of the theoretical calculations

ACD/ChemSketch (Advanced Chemistry Development, Inc., Toronto, Ontario, Canada) was used for the 2D chemical drawing of all of the molecules and then, using these structures, various in silico ADME and drug-likenesses properties of the molecules were examined using the SwissADME webserver[59,60] (Swiss Institute of Bioinformatics, Lausanne, Switzerland). Next, 2D structures of the molecules were converted into 3D structures in Protein Data Bank format using Open Babel[61], and subsequently, their energy was optimized using Avogadro v.1.2.0[62] (http://avogadro.cc/). Afterwards, these optimized molecules and target structures were prepared for docking simulations using the PyRx program.[63] Herein, the crystal structure of a sterol 14α-demethylase (CYP51) for the cytochrome P450 enzyme (PDB ID: 5TZ1[32]) was used as the target structure. Finally, the docking simulations were performed using AutoDock Vina software[64] (Scripps Research, San Diego, California) with the Lamarckian genetic algorithm (LGA).[65,66] Moreover, Discovery studio (Dassault Systèmes Biovoda, Vélizy-Villacoublay, France) and Maestro software (Schrödinger, New York, New York) were used for visualizations of the docking results.

ACKNOWLEDGMENTS

The authors would like to thank Karabuk University (KBU-BAP-16/2-YL-090) for their support in funding this research.

DATA AVAILABILITY STATEMENT

The data that support the findings of this study are openly available in [Supplementary Material] at http://doi.org/[doi], reference number [reference number].

ORCID

Mustafa Er https://orcid.org/0000-0002-0868-2101
Hakan Tahtaci https://orcid.org/0000-0002-1557-6315

REFERENCES

[1] H. Tahtaci, H. Karacık, A. Ece, M. Er, M. G. Şeker, *Mol. Inform.* **2018**, *37*, 1700083.
[2] M. L. Fascio, C. S. Sepúlveda, E. B. Damonte, N. B. D'Accorso, *Carbohydr. Res.* **2019**, *480*, 61.
[3] M. Bakherad, S. Karami, A. Keivanloo, S. Sepehri, *ChemistrySelect* **2018**, *3*, 11042.
[4] D. M. Egorov, Y. L. Piterskaya, A. V. Dogadina, N. I. Svintsitskaya, *Tetrahedron Lett.* **2015**, *56*, 1552.
[5] R. Yi, S. Liu, H. Gao, Z. Liang, X. Xu, N. Li, *Tetrahedron* **2020**, *76*, 130951.
[6] D. G. Daraji, D. P. Rajani, S. D. Rajani, E. A. Pithawala, S. Jayanthi, H. D. Patel, *Bioorg. Med. Chem. Lett.* **2021**, *36*, 127819.
[7] I. Amine Khodja, H. Boulebd, C. Bensouici, A. Belfaitah, *J. Mol. Struct.* **2020**, *1218*, 128527.
[8] E. M. H. Ali, M. S. Abdel-Maksoud, U. M. Ammar, K. I. Mersal, K. Ho Yoo, P. Jooryeong, C.-H. Oh, *Bioorg. Chem.* **2021**, *106*, 104508.
[9] V. Ji Ram, A. Sethi, M. Nath, R. Pratap, *The Chemistry of Heterocycles*, 1st ed., Elsevier, Amsterdam **2019**.
[10] Y. Luo, S. Zhang, Z.-J. Liu, W. Chen, J. Fu, Q.-F. Zeng, H.-L. Zhu, *Eur. J. Med. Chem.* **2013**, *64*, 54.
[11] A. A. Kadi, N. R. El-Brollosy, O. A. Al-Deeb, E. E. Habib, T. M. Ibrahim, A. A. El-Emam, *Eur. J. Med. Chem.* **2007**, *42*, 235.
[12] K. Sancak, Y. Ünver, M. Er, *Turk. J. Chem.* **2007**, *31*, 125.
[13] A. Skrzypek, J. Matysiak, M. Karpińska, K. Czarnecka, P. Kręcisz, D. Stary, J. Kukułowicz, B. Paw, M. Bajda, P. Szymański, A. Niewiadomy, *Bioorg. Chem.* **2021**, *107*, 104617.
[14] W. S. Alwan, R. Karpoormath, M. B. Palkar, H. M. Patel, R. A. Rane, M. S. Shaikh, A. Kajee, K. P. Mlisana, *Eur. J. Med. Chem.* **2015**, *95*, 514.
[15] I. A. M. Khazi, A. K. Gadad, R. S. Lamani, B. A. Bhongade, *Tetrahedron* **2011**, *67*, 3289.
[16] T. Zarganes-Tzitzikas, C. G. Neochoritis, J. Stephanidou-Stephanatou, C. A. Tsoleridis, G. Buth, G. E. Kostakis, *Tetrahedron* **2013**, *69*, 5008.
[17] S. G. Alegaon, K. R. Alagawadi, *Eur. J. Chem.* **2011**, *2*, 94.
[18] B. Chandrakantha, A. M. Isloor, P. Shetty, H. K. Fun, G. Hegde, *Eur. J. Med. Chem.* **2014**, *71*, 316.
[19] K. F. M. Atta, O. O. M. Farahat, A. Z. A. Ahmed, M. G. Marei, *Molecules* **2011**, *16*, 5496.
[20] V. B. Jadhav, M. V. Kulkarni, V. P. Rasal, S. S. Biradar, M. D. Vinay, *Eur. J. Med. Chem.* **2008**, *43*, 1721.
[21] J. Ramprasad, N. Nayak, U. Dalimba, P. Yogeeswari, D. Sriram, *Bioorg. Med. Chem. Lett.* **2015**, *25*, 4169.
[22] J. Ramprasad, N. Nayak, U. Dalimba, P. Yogeeswari, D. Sriram, S. K. Peethambar, R. Achur, H. S. S. Kumar, *Eur. J. Med. Chem.* **2015**, *95*, 49.
[23] S. G. Alegaon, K. R. Alagawadi, P. V. Sonkusare, S. M. Chaudhary, D. H. Dadwe, A. S. Shah, *Bioorg. Med. Chem. Lett.* **2012**, *22*, 1917.
[24] S. Cascioferro, G. L. Petri, B. Parrino, D. Carbone, N. Funel, C. Bergonzini, G. Mantini, H. Dekker, D. Geerke, G. J. Peters, G. Cirrincione, E. Giovannetti, P. Diana, *Eur. J. Med. Chem.* **2020**, *189*, 112088.
[25] B. A. Bhongade, S. Talath, R. A. Gadad, A. K. Gadad, *J. Saudi Chem. Soc.* **2016**, *20*, S463.

[26] S. Kumar, B. Metikurki, V. S. Bhadauria, E. Clercq, D. Schols, H. Tokuda, S. S. Karki, *Acta Pol. Pharm.* **2016**, *73*, 913.
[27] E. Taflan, H. Bayrak, M. Er, Ş. A. Karaoğlu, A. Bozdeveci, *Bioorg. Chem.* **2019**, *89*, 102998.
[28] R. Romagnoli, P. G. Baraldi, F. Prencipe, J. Balzarini, S. Liekens, F. Estévez, *Eur. J. Med. Chem.* **2015**, *101*, 205.
[29] M. P. Narasimha Rao, B. Nagaraju, J. Kovvuri, S. Polepalli, S. Alavala, M. V. P. S. Vishnuvardhan, P. Swapna, V. D. Nimbarte, J. K. Lakshmi, N. Jain, A. Kamal, *Bioorg. Chem.* **2018**, *76*, 420.
[30] R. Roskoski Jr., *Pharmacol. Res.* **2015**, *100*, 1.
[31] S. Kumar, V. Gopalakrishnan, M. Hegde, V. Rana, S. S. Dhepe, S. A. Ramareddy, A. Leoni, A. Locatelli, R. Morigi, M. Rambaldi, M. Srivastava, S. C. Raghavan, S. S. Karki, *Bioorg. Med. Chem. Lett.* **2014**, *24*, 4682.
[32] T. Y. Hargrove, L. Friggeri, Z. Wawrzak, A. Qi, W. J. Hoekstra, R. J. Schotzinger, J. D. York, F. P. Guengerich, G. I. Lepesheva, *J. Biol. Chem.* **2017**, *292*, 6728.
[33] M. Er, G. Isildak, H. Tahtaci, T. Karakurt, *J. Mol. Struct.* **2016**, *1110*, 102.
[34] M. Er, A. M. Abounakhla, H. Tahtaci, A. H. Bawah, S. S. Çınaroğlu, A. Onaran, A. Ece, *Chem. Cent. J.* **2018**, *12*, 121.
[35] M. Er, F. Ahmadov, T. Karakurt, Ş. Direkel, H. Tahtaci, *ChemistrySelect* **2019**, *4*, 14281.
[36] M. Er, H. Tahtaci, T. Karakurt, A. Onaran, *J. Heterocycl. Chem.* **2019**, *56*, 2555.
[37] M. Er, B. Ergüven, H. Tahtaci, A. Onaran, T. Karakurt, A. Ece, *Med. Chem. Res.* **2017**, *26*, 615.
[38] M. Er, A. Şahin, H. Tahtacı, *Maced. J. Chem. Chem. Eng.* **2014**, *33*, 189.
[39] M. Er, A. Özer, Ş. Direkel, T. Karakurt, H. Tahtaci, *J. Mol. Struct.* **2019**, *1194*, 284.
[40] S. S. Karki, K. Panjamurthy, S. Kumar, M. Nambiar, S. A. Ramareddy, K. K. Chiruvella, S. C. Raghavan, *Eur. J. Med. Chem.* **2011**, *46*, 2109.
[41] A. Sowmya, G. N. Anil Kumar, S. Kumar, S. S. Karki, *Chem. Data Collect.* **2020**, *25*, 100326.
[42] H. Tahtaci, M. Er, T. Karakurt, K. Sancak, *Tetrahedron* **2017**, *73*, 4418.
[43] A. K. Ghose, V. N. Viswanadhan, J. J. Wendoloski, *J. Comb. Chem.* **1999**, *1*, 55.
[44] W. J. Egan, K. M. Merz, J. J. Baldwin, *J. Med. Chem.* **2000**, *43*, 3867.
[45] D. F. Veber, S. R. Johnson, H.-Y. Cheng, B. R. Smith, K. W. Ward, K. D. Kopple, *J. Med. Chem.* **2002**, *45*, 2615.
[46] I. Muegge, S. L. Heald, D. Brittelli, *J. Med. Chem.* **2001**, *44*, 1841.
[47] F. Lovering, J. Bikker, C. Humblet, *J. Med. Chem.* **2009**, *52*, 6752.
[48] W. Wei, S. Cherukupalli, L. Jing, X. Liu, P. Zhan, *Drug Discovery Today* **2020**, *25*, 1839.
[49] F. Lovering, *MedChemComm* **2013**, *4*, 515.
[50] C. A. Lipinski, F. Lombardo, B. W. Dominy, P. J. Feeney, *Adv. Drug Delivery Rev.* **1997**, *23*, 3.
[51] G. Sheldrick, *Acta Crystallogr. Sect. A* **2015**, *71*, 3.
[52] G. M. Sheldrick, Crystal structure refinement with SHELXL *Acta Crystallographica Section C Structural Chemistry* **2015**, *71*, 3. http://dx.doi.org/10.1107/s2053229614024218.
[53] O. V. Dolomanov, L. J. Bourhis, R. J. Gildea, J. A. K. Howard, H. Puschmann, *J. Appl. Crystallogr.* **2009**, *42*, 339.
[54] C. F. Macrae, P. R. Edgington, P. McCabe, E. Pidcock, G. P. Shields, R. Taylor, M. Towler, J. van de Streek, *J. Appl. Crystallogr.* **2006**, *39*, 453.
[55] J.-H. Byun, Y. Seo, D. Kim, M. Kim, H. Lee, D. Yong, K. Lee, Y. Chong, *J. Microbiol. Methods* **2020**, *168*, 105781.
[56] D. Pandey, N. Tripathi, R. Tripathi, S. Dixit, *Z. Pflanzenkr. Pflanzenschutz* **1982**, *89*, 344349.
[57] M. Chandrasekaran, V. Venkatesalu, *J. Ethnopharmacol.* **2004**, *91*, 105.
[58] K. S. Babu, X.-C. Li, M. R. Jacob, Q. Zhang, S. I. Khan, D. Ferreira, A. M. Clark, *J. Med. Chem.* **2006**, *49*, 7877.
[59] A. Daina, O. Michielin, V. Zoete, *Sci. Rep.* **2017**, *7*, 42717.
[60] A. Daina, O. Michielin, V. Zoete, *J. Chem. Inf. Model.* **2014**, *54*, 3284.
[61] N. M. O'Boyle, M. Banck, C. A. James, C. Morley, T. Vandermeersch, G. R. Hutchison, *Aust. J. Chem.* **2011**, *3*, 33.
[62] M. D. Hanwell, D. E. Curtis, D. C. Lonie, T. Vandermeersch, E. Zurek, G. R. Hutchison, *Aust. J. Chem.* **2012**, *4*, 17.
[63] S. Dallakyan, A. J. Olson, *Chemical Biology: Methods and Protocols*, Springer, New York, NY **2015**.
[64] O. Trott, A. J. Olson, *J. Comput. Chem.* **2010**, *31*, 455.
[65] F. J. Solis, R. J. B. Wets, *Math. Oper. Res.* **1981**, *6*, 19.
[66] R. Huey, G. M. Morris, A. J. Olson, D. S. Goodsell, *J. Comput. Chem.* **2007**, *28*, 1145.

SUPPORTING INFORMATION

Additional supporting information may be found online in the Supporting Information section at the end of this article.

How to cite this article: Tunel H, Er M, Alici H, Onaran A, Karakurt T, Tahtaci H. Synthesis, structural characterization, biological activity, and theoretical studies of some novel thioether-bridged 2,6-disubstituted imidazothiadiazole analogues. *J Heterocyclic Chem*. 2021;58:1321–1343. https://doi.org/10.1002/jhet.4260